ELSEVIER

Physica A 287 (2000) 49–82

PHYSICA A

www.elsevier.com/locate/physa

Multifractal absolute galactic luminosity distributions and the multifractal Hubble 3/2 law

S. Lovejoy[a,*], P. Garrido[a], D. Schertzer[b]

[a] *Department of Physics, McGill University, 3600 University St., Montréal, Québec, Canada H3A 2T8*
[b] *LMM (CNRS) Boite 162, Université P.& M. Curie, 4 Pl. Jussieu, Paris 75252 Cedex 05, France*

Received 16 August 1999

Abstract

Scale-invariant intergalactic dynamics governed by a statistically homogeneous cascade process generically yields multifractal luminosity distributions with highly inhomogeneous realizations (the standard nonfractal and fractal models are special limiting cases). The main obstacles for extending scaling analyses to the spatial distribution of galactic absolute luminosities are the large "Malmquist" catalogue biases which – for multifractal galaxy distributions – we here show how to remove. We also derive the theoretical relation between absolute and apparent luminosity multifractal catalogues (the multifractal extension of the "Hubble 3/2" law; not to be confused with the more usual Hubble law governing the expansion of the universe) and show that the theory is compatible with both the observed apparent and absolute luminosities. The results of multifractal analysis on two galaxy catalogues (depth 150 h^{-1} Mpc each) show that the observed form of the dimension function follows if only matter in sufficiently dense (and sparse) concentrations is luminous (with critical dimension $D_c \approx 1.85$), i.e., mass and luminosity are tightly correlated only above a critical mass density singularity threshold ($\gamma_c \approx 0.4$). Since this critical singularity is considerably larger than that which determines the mean mass, the clusters responsible for the mean mass are dark and we obtain a "dark mass exponent" $\delta \approx 0.75$. This implies that the ratio of luminous to dark matter is Λ'^{δ} where Λ' is the ratio of the outer and inner cascade scales; taking Λ' in the range 10–100 we find that 85–97% of the matter is dark ($\Lambda' \approx 10$ is the value most compatible with the microwave background and standard cosmologies and with the data used here, $\Lambda' \approx 100$ is apparently compatible with some galaxy catalogues). The model also includes a multifractal phase transition associated with very bright self-organized critical galaxies whose luminosity we find to be algebraic with critical exponent ≈ 4 (not exponential as is often assumed). A basic problem with the scaling models proposed to date is that there is no satisfactory way of reconciling the high heterogeneity of luminous matter (fractal dimension $\leqslant 1.85$) with the apparently low heterogeneity of the mass as inferred from the cosmic background or the small peculiar velocities. Our model concretely shows that the fractal dimension of the regions making the dominant contribution to the mean density may be as large as $D_1 \approx 2.97$ which is very close to the space filling value 3. We show that this may give deviations from the Hubble law as small as 3–7% (for $\Lambda' = 10$), as required by the observations.

Keywords: Fractal; Multifractal galaxy number counts; Fractal universe; Large-scale structure of the universe; Hubble 3/2 law

* Corresponding author.

0378-4371/00/$ - see front matter
PII: S0378-4371(00)00247-8

1. Introduction

1.1. The outer scale of mass cascades and the "de Vaucouleurs–Hubble" paradox

The evolution of the universe is governed by gravitational and electromagnetic forces both of which are power-law functions with no characteristic lengths. It is therefore natural to assume that the statistics of the distribution of matter and luminosity are scale invariant over wide ranges of scale. If we hypothesize a scale-invariant cascade of nonlinear interactions/instabilities this will lead (generically [1]) to multifractal distributions of galactic mass and luminosity; hence the relevance of a large number of empirical studies testing the scaling properties and limits of galaxy distributions. As data have improved, the outer (homogeneity) scale of the scaling has been pushed out further and further, with a recent review [2] concluding that the outer scale may be as large as 1000 h^{-1} Mpc (h is the Hubble parameter; $h = 1$ corresponds to a Hubble constant $H_0 = 100\,\mathrm{km\,s^{-1}\,Mpc^{-1}}$.). In contrast, numerous studies showing relatively small heterogeneity in the microwave background (especially COBE) coupled with standard models such as the cold dark matter model have led to a tightening upper bound on the scaling regime; specifically, they are interpreted as showing the universe to be homogeneous over scales larger than ≈ 100–$150\ h^{-1}$ Mpc. For example, Fig. 1 shows a recent power spectral density $P(k)$ adapted from Ref. [3] which compares the (favoured) cold and hot dark matter model with a wide variety of observations. The spectral peak corresponding to ≈ 100–$200\ h^{-1}$ Mpc is probably the largest outer scale compatible with these (indirect) observations of mass density fluctuations, and is the scale imposed by the finite age of the universe coupled with the estimated expansion rate (it is the size of the horizon at the time that the density of matter and radiation were equal). In comparison, the inner scale would be at least as small as the mean intergalactic distance ($\approx 10\ h^{-1}$ Mpc); hence scale ratios Λ (largest/smallest) could be at least 15–20.

If the disagreement in the outer scales was the only problem, given the uncertainties in both data and theories, it would probably not be serious. However, the scaling studies of galaxy catalogues have shown that the heterogeneity in the luminous matter is enormous; even intrinsically dim galaxies apparently are distributed on very sparse sets which have fractal dimensions of ≈ 1.85–2 or less. As Sylos Labini et al. [2] have pointed out, if mass tracks the luminosity, then this implies that density fluctuations are also enormous. This implies peculiar velocities so large that it becomes impossible to explain how the Hubble law accurately holds down to distances as small as several Mpc (as observed). It is probable that this apparent implication of the scaling observations for mass densities that Sylos Labini et al. [2] call the "de Vaucouleurs–Hubble paradox" has led to the latter being largely ignored by mainstream cosmology.

In this paper, we propose a possible resolution of this contradiction based on the systematic application of scaling (i.e., multifractal) notions. By analysing two galaxy catalogues (each 150 h^{-1} Mpc deep; carefully correcting for the range-dependent biases), we show that a simple model can explain all the observations. The key assumption of the model is simply that only sufficiently dense mass concentrations will be luminous;

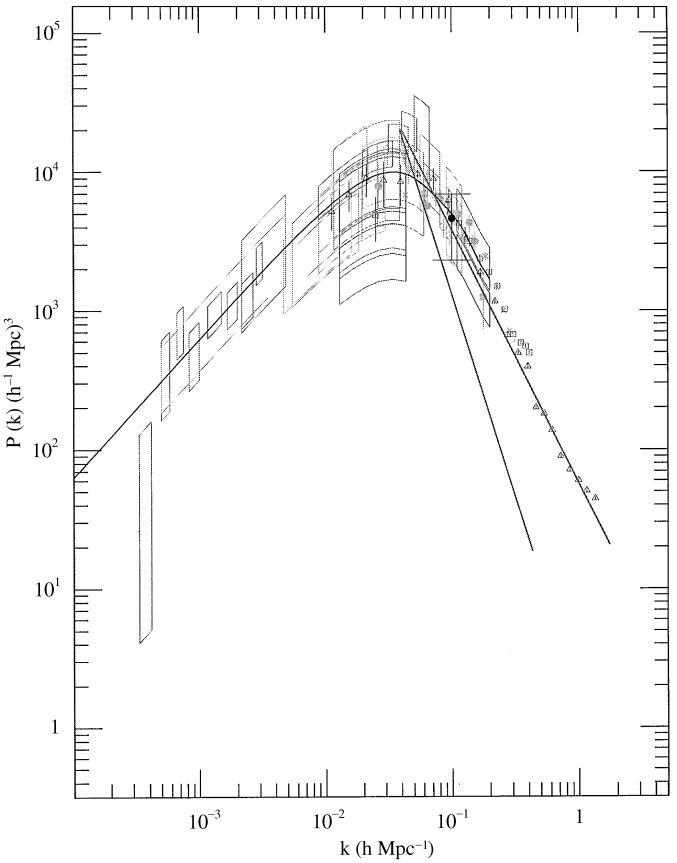

Fig. 1. The spectral density of the mass density estimated from cosmic microwave background measurements (boxes bounded above and below by two standard deviation limits), the cold and hot dark matter model (curved line), and galaxy catalogues (APM survey (triangles), Las Campanas (squares), IRAS (circles), SSRS2+CfA2 (crosses); adapted from Ref. [3]. Also shown are two straight lines with absolute slopes $s_{\mathscr{L}} = 1.85$, $s_\rho = 2.93$ which are the luminosity and mass density spectral densities of the thresholded multifractal model discussed here (with outer scale $150\,h^{-1}$ Mpc; slightly better fit is obtained at 100 h^{-1} Mpc). The s_ρ value assumes the lognormal multifractal for the mass density; for $\alpha < 2$, s_ρ lies between this extreme and $s_{\mathscr{L}}$ (i.e., any scaling spectra lying between the straight lines indicated are compatible with the data).

mass tracks luminosity only above a critical singularity ($\gamma_c \approx 0.4$ corresponding to a critical fractal dimension of about 1.85). Density singularities below γ_c will be concentrated on (generally) fractal sets with dimensions less than the space filling value 3; they will still be sparse but to a lesser degree [it is possible that some finite γ exists which is not fractal (i.e., with $D = 3$). Alternatively, the only truly space-filling component of the density field may be the limit of a perfect vacuum: $D(\gamma) \to 3$ as $\gamma \to -\infty$]. We quantitatively show that the critical dimension associated with the mean density can be as large as 2.97 which we show gives acceptably small peculiar velocities. The impact of this "nontracking" of the nonextreme mass concentrations and luminosity implies that the spectral exponents of the two are quite different; Fig. 1 shows the

very different spectra of mass density and luminosity that this would imply. Finally, the model also implies that most of the mass is dark (at least 85%; depending on the outer scale), implying values of the density parameter Ω greater than 0.1 (depending sensitively on Λ').

1.2. Cascade properties

Although the nonlinear processes governing the mass cascade are statistically homogeneous and hence respect a statistical version of the cosmological principle (i.e., they are statistically translationally invariant), individual realizations are highly inhomogeneous. If, in addition to respecting a scaling symmetry, the cascades are statistically isotropic, they are termed "self-similar". More generally, the cascades may only respect an anisotropic scaling symmetry – "generalized scale invariance" [5];[1] they are scaling multifractals but are not self-similar.

Let us now consider a cascade of mass density (a priori, this would include the total baryonic and nonbaryonic mass) associated with a hierarchy of instabilities. It is now known that cascades generically yield the following[2] nonclassical statistical behaviour:

$$\langle \rho_\Lambda^q \rangle = \Lambda^{K_\rho(q)} . \tag{1}$$

Λ is the corresponding scale ratio (large scale/small scale; $\Lambda > 1$, see Section 2), ρ_Λ is the (dimensionless) ratio of mass density at the scale ratio Λ divided by the (ensemble) mean density; and $K_\rho(q)$ is the moment scaling function. In the following Λ indicates the catalogue scale ratio, Λ' the scale ratio of the cascade process itself, and λ the cascade ratio of volume limited sub-catologues. For a monofractal mass distribution, $K_\rho(q)$ is linear; more generally, it will be nonlinear and convex. The relationship between ρ_Λ and the corresponding nondimensional mass (m_Λ) is

$$m_\Lambda = \rho_\Lambda \Lambda^{-d} , \tag{2}$$

since Λ^{-d} is the corresponding volume ratio ($d = 3$, is the dimension of space). Equivalently, rather than specifying the statistical properties via the statistical moments (Eq. (1)), we can specify them via probabilities [6]

$$\Pr(\rho'_\Lambda > \Lambda^{\gamma_\rho}) \approx \Lambda^{-c_\rho(\gamma_\rho)} ,$$

$$\gamma_\rho = \frac{\log \rho_\Lambda}{\log \Lambda} , \tag{3}$$

[1] In general, the scale changing operator relating small and large scales can involve differential stratification, rotation or more general transformations; in Ref. [4] it was suggested that galaxies may be classified with the help of generalized scale invariance. The isotropy of the large-scale universe would follow if the outer cascade scale was statistically isotropic even though; the scale changing operator itself could involve preferred directions, since these would only imply anisotropy of smaller scale structures. Hence, we need not assume a priori that the multifractal cascade is itself self-similar (i.e., scaling and isotropic).

[2] The difference between isotropic and anisotropic scaling is in the definition of the scale and scale ratio λ; the theoretical formulae used throughout the introduction do not presuppose isotropy. The latter is, however, implicitly assumed in the data analysis section, both the method of defining subcatalogues and that of estimating the scale ratios.

where ρ'_Λ is a randomly chosen density at resolution Λ; ρ_Λ is a density threshold which is related to the corresponding singularity γ_ρ in the manner indicated, "Pr" indicates "probability", $c_\rho(\gamma_\rho)$ is the codimension function of the mass density, and the equality "$\approx$" in Eq. (3) is to within slowly varying factors such as $\log \Lambda$ terms. If d is the dimension of space, whenever $c_\rho(\gamma_\rho) \leqslant d$, there is a simple geometric interpretation:[3] $D_\rho(\gamma_\rho) = d - c(\gamma_\rho)$ where $D_\rho(\gamma_\rho)$ is the fractal dimension of the set whose mass density exceeds Λ^{γ_ρ}. The two descriptions $c_\rho(\gamma_\rho)$, $K_\rho(q)$ are related via a Legendre transform as

$$K_\rho(q) = \max_{\gamma_\rho} [q\gamma_\rho - c_\rho(\gamma_\rho)] ,$$

$$c_\rho(\gamma) = \max_{q} [q\gamma_\rho - K_\rho(q)] . \tag{4a}$$

This Legendre relation (exactly valid in the limit $\Lambda \to \infty$) has fundamental consequences since it implies that there is a one-to-one relationship between orders of singularity γ_ρ and moments q:

$$q = c'_\rho(\gamma_\rho) ,$$

$$\gamma_\rho = K'_\rho(q) . \tag{4b}$$

This means that only a single fractal set (with codimension $c_\rho(K'_\rho(q))$) gives the overwhelmingly dominant contribution to the qth-order moment.

In order for the cascade to have a well-defined small-scale limit, there must be a quantity conserved scale by scale as the cascade proceeds. Assuming for the moment that it is the mass density which is conserved,[4] we obtain

$$\langle \rho_\Lambda \rangle = constant , \quad K_\rho(1) = 0 , \tag{5}$$

i.e., $\langle \rho_\Lambda \rangle \propto \Omega$ (the density parameter, i.e., the usual density nondimensionalized by the critical density needed to close the universe). Note that Eq. (5) states only that the ensemble mean density is independent of resolution; it is a statement of scale-by-scale mean conservation, not spatial homogeneity, it by no means implies that the density of any realization of the process is homogeneous. On the contrary, the dominant contribution to the mean density is due to a sparse fractal set with dimension denoted by $D_1 = d - C_1$ below ($d = 3$, $C_1 = K'_\rho(1)$; see Eq. (4)).

The scale-by-scale conservation of mass density (Eq. (5)) is theoretically appealing since it would imply that the (ensemble) mean mass would have "trivial" scaling (proportional to the volume of space); it would be the fundamental cascade quantity. If in addition, the corresponding C_1 is small enough (the limit $C_1 = 0$ corresponds to spatial homogeneity on each realization), this would allow – in accordance with

[3] This is a major advantage of the statistical codimension formalism of multifractals; $c(\gamma)$ is always $\geqslant 0$ whereas when $c(\gamma) > d$; $D(\gamma) < 0$ and so it cannot be interpreted as a geometric dimension.

[4] We are really considering the constancy of the flux of mass density from large to small scales during the cascade and supposing that the mean density is independent of scale. This scale-by-scale conservation is an additional hypothesis; it does not follow directly from the law of conservation of mass.

observations – the Hubble law to be accurately linear even at small scales.[5] Indeed, Sylos Labini et al. [2] have pointed out that if instead the mass distribution follows that of the luminosity field (which they argue is fractally scaling with $D \approx 2$ out to the largest observed scales, i.e., at least 1000 h^{-1} Mpc), that it would lead to a "de Vaucouleurs–Hubble" paradox, i.e., to an apparent contradiction between the scaling and the Hubble law. Indeed, there is a large literature on the relation between galaxy absolute luminosity (L) and mass (m; see e.g. Ref. [7] for a review), the empirical evidence favours a power-law relation of the form

$$L \propto m^n, \quad \mathscr{L} \propto \rho^\eta ,$$
$$L_\Lambda = \mathscr{L}_\Lambda \Lambda^{-d} , \tag{6}$$

where $\mathscr{L}$ is the luminosity per unit volume and empirically the exponent η is close to unity. If $\eta = 1$, then we obtain

$$c_{\mathscr{L}}(\gamma_{\mathscr{L}}) = c_\rho(\gamma_\rho), \quad \gamma_{\mathscr{L}} > \gamma_{\mathscr{L}c} ,$$
$$\gamma_{\mathscr{L}} = \gamma_\rho , \tag{7}$$

where $\gamma_{\mathscr{L}c}$ is a critical order of singularity. In our model, for $\gamma_{\mathscr{L}} < \gamma_{\mathscr{L}c}$, $c_{\mathscr{L}}(\gamma_{\mathscr{L}})$ and $c_\rho(\gamma_\rho)$ will be different, with $c_{\mathscr{L}}(\gamma_{\mathscr{L}}) = C_c$ = constant whereas $c_\rho(\gamma_\rho)$ continues to decline as γ_ρ decreases. This could arise since for $\gamma_{\mathscr{L}} < \gamma_{\mathscr{L}c}$ the density is not high enough for galaxy formation, i.e., the corresponding density structures are dark. As we see below, not only does this model avoid the de Vaucouleurs–Hubble paradox, but also has the added bonus of automatically and quantitatively accounting for the missing mass: the latter is simply hiding in dark clusters.[6]

Although Sylos Labini et al. [2] do consider the possibility of a multifractal distribution of mass, they do not directly connect this to a possible resolution of the de Vaucouleurs–Hubble paradox as we do here. Instead, they give two extreme alternatives neither of which they judge satisfactory. In alternative 1, they propose a truly homogeneous dark matter distribution completely uncorrelated with the galaxies, arguing (using linear perturbation theory) that it would have to have a density very near the critical density for flat space-time in order to explain small variations about the Hubble law. In alternative 2, the matter and galaxies are completely tied together and the Hubble law results from a totally different mechanism such as a cosmological gravitational redshift. In comparison, our model (backed up by empirical data below) which assumes

[5] The "drift" in the mean of many fractal models is due to their nonstationarity/nonhomogeneity. In contrast, all the cascade processes are by construction homogeneous (statistically translationally invariant) out to their outer scales. However, if the mean is not conserved, then they will nevertheless display apparent nonhomogeneity/"drift" on individual realizations for scales smaller than their outer scale. The wide range validity of the Hubble law limits this apparent nonhomogeneity; of more relevance to the validity of the Hubble law is the heterogeneity of the density levels which give the dominant contribution to the spatial means on single realizations, i.e., those with critical orders of singularity $\gamma_1 = K'_\rho(1)$. For conservative multifractal densities, $\gamma_1 = C_1 = K'_\rho(1)$ where C_1 is the codimension of the density level which gives the dominant contribution to the mean. In Section 5, we show that this can easily be as small as 0.03 ($D_1 = d - C_1 = 2.97$) whereas the codimension of the support of the luminosity is $C_c \approx 1.15$ which is quite large; $D_c = d - C_c = 1.85$.

[6] This could be either baryonic or non-baryonic matter. We readily obtain factors of 10–100; see Section 5.

only that mass and luminosity are tightly correlated above a minimum threshold can be understood as a kind of compromise between the two alternatives. This is because on the one hand, the high-order mass density singularities are indeed associated with the galaxies (which however only contribute a small fraction to the total mass), while on the other hand, the galaxies themselves are embedded inside (and hence are subtly correlated with) the lower-order (dark matter) singularities which dominate the mean mass and hence the Hubble law.

1.3. Galaxy number counts

Since the number distribution and the probability are related by a factor equal to the volume of space at the inner cascade scale (Λ^{-d}), we obtain the following galactic number distribution:

$$N(L_\Lambda) = \Lambda^d \Pr(L'_\Lambda > \Lambda^\gamma) \approx \Lambda^{D(\gamma)} ,$$
$$\gamma = \frac{\log L_\Lambda}{\log \Lambda} . \tag{8a}$$

$N(L_\Lambda)$ is the number of galaxies brighter than the nondimensional absolute luminosity L_Λ.[7] In standard notation, if we had a perfect (unbiased) catalogue, using the luminosity function $\phi(L')$ [the number of galaxies per unit volume with absolute luminosity between L and $L + \mathrm{d}L$], we have

$$N(L_\Lambda) = \int_{L_\Lambda}^{\infty} \phi(L')\,\mathrm{d}L' . \tag{8b}$$

Note that we integrate over the brightest and not the dimmest galaxies. Below, using this unbiased number distribution, we calculate the volume-limited catalogue number distributions (the precise result is given by Eq. (32) if we incorporate the singularity shift given in Eq. (42)).

At the most general level, the only constraint on $D(\gamma)$ is that it is a concave function; however, under rather general circumstances it falls into universality classes governed by three basic parameters [6]. In addition, of direct relevance here, for general "canonical" cascades, there exists a generic behaviour of the extreme singularities; $D(\gamma)$ will become linear (the "multifractal phase transition route" to self-organized criticality; see Refs. [8,9]):

$$D(\gamma) = (\gamma_s - \gamma) q_D, \quad \gamma \geqslant \gamma_D , \tag{9}$$

where γ_s, γ_D and q_D are constants; $D(\gamma)$ is concave for $\gamma < \gamma_D$. This behaviour (which corresponds to a multifractal phase transition at $\gamma = \gamma_D$) leads to the divergence of statistical moments of order $\geqslant q_D$. Since almost surely, no sets with $D < 0$ can be observed, γ_s corresponds to the highest singularity (the luminosity of the brightest galaxy $L_{\Lambda,\max} = \Lambda^{\gamma_s}$, i.e., it depends on the catalogue depth in a power-law manner) observable in any given realization (more extreme values corresponding to negative D

[7] In Section 2, we carefully distinguish biased and unbiased GNCs.

will only be observed on an ensemble with many realizations). Finally, in our model only sufficiently high concentrations of mass are luminous (i.e., corresponding to $\gamma > \gamma_c$ for some critical γ_c), and if in addition we suppose that $\gamma_D < \gamma_c$, then we obtain the thresholded model

$$D(\gamma) = D(\gamma_c) = D_c, \quad \gamma < \gamma_c\,, \tag{10a}$$

$$D(\gamma) = (\gamma_s - \gamma) q_D, \quad \gamma > \gamma_c\,. \tag{10b}$$

This combination of linear "tail" and constant multifractal "filter" at γ_c is indeed close to the catalogues analysed here.[8]

Up until now, the only scaling *models* (for analyses, see the next section) for the absolute luminosity have been the nonfractal and monofractal models [11–14].[9] These are the special cases where

$$D(\gamma) = D_c, \quad \gamma < \gamma_c\,, \tag{11a}$$

$$D(\gamma) = -\infty, \quad \gamma \geqslant \gamma_c\,, \tag{11b}$$

in which $0 \leqslant D_c \leqslant d$ is the dimension[10] of the mean luminosity. The nonfractal model is not only generated by a homogeneous process, in addition, each realization is homogeneous: it has $D_c = d$ (the dimension of space, here $d = 3$). The fractal model (corresponding to a "β model" in turbulence) is generated by a homogeneous process but already has highly inhomogeneous realizations: $D_c < d$, hence it is sparse at all scales. Note that Eq. (11b) is a special case of Eq. (9) with $q_D = \infty$. Eqs. (11a) and (11b) imply that over a fractal set with dimension D_c the distribution of luminosities is arbitrary (this is a fractal generalisation of the standard assumption that the galaxy luminosity is statistically independent of its location). In contrast, the multifractal model involves subtle long-range correlations between the location and luminosity because it predicts that the brightest galaxies are sparser (more clustered) than the dimmer ones ($D(\gamma)$ is generally a decreasing and concave function).

1.4. Empirical tests of multifractal luminosities; D-biases and γ-biases

Although Eq. (8) is a general prediction for scale-invariant dynamics, it has not yet been directly empirically tested on absolute luminosities. So far, multifractal analyses of galaxy catalogues have been limited to the following:

[8] Strictly speaking, the model presented here is thresholded in D, not γ. However, the thresholding of a "bare" cascade process at the finest cascade resolution would result in a thresholding of the lower resolution (spatially averaged) "dressed" cascade in D, see Ref. [10].

[9] Note that many multifractal analyses have been made of the galaxy number density (see Refs. [15–17]), which can quantify the spatial clustering. However, this is a totally different multifractal measure (the multifractality of the "support"); it is not trivially related to the multifractal measure defined by the absolute luminosities, and which – as we show below – is related to the mass distribution.

[10] All the dimensions discussed here are correlation dimensions because they are statistical exponents obtained by averaging over special locations (galaxy centres) rather than over arbitrary centres. The usual ("box") dimensions are lower bounds; Ref. [18] shows that for apparent luminosities there is a significant difference between the two.

(a) *The multifractal measure defined by the number density of galaxies*, or equivalently, the multifractality of the "support" [17,18]. As pointed out in Refs. [18–20], the number density per se has little physical significance, so we will not pursue this here; as we see below, suffice it to say that in general, if the absolute luminosities are multifractal (Eq. (1)), then the number density estimates will themselves have range-dependent biases that are best accounted for knowing the multifractal properties of L.

(b) *The multifractal measure defined by the apparent luminosities* (ℓ; [18] treats an infinite family of measures obtained by raising ℓ to various powers: ℓ^{η}). The advantage of using ℓ is that – as long as the catalogue is unbiased for all *apparent* luminosities greater than a threshold – there are no range-dependent effects. Indeed, in Ref. [18] excellent scaling was obtained up to the largest available angles (in the 1-D projection of the CfA2 catalogue; up to angles of $\approx 100^{\circ}$, see Section 3). The disadvantage of this approach is that the physical significance of the apparent luminosity dimension function is unclear, and as pointed out in Ref. [21], and Section 4, the statistics suffer large fluctuations (due to the strong $1/r^2$ fall-off in apparent luminosity) when the apparent luminosities are determined at various locations (these can, however, be dealt with either by reprojecting [18], or using double volume-limited catalogues (see Ref. [21], and text below)).

(c) *The multiscaling of the moments of the uncorrected (biased) absolute luminosity catalogues*: In Ref. [20] the multifractal measure defined by L was used but with two important differences with respect to the approach used here. First, the data were gridded to estimate the luminosities at a degraded resolution L_{λ} ($\lambda < \Lambda$). Then, the sum over the qth-order statistical moments was estimated:

$$\sum_{i=1}^{\lambda^d} L_{\lambda,i}^{q} = \lambda^{-\tau(q)} \approx \lambda^{d} \langle L_{\lambda}^{q} \rangle \,. \tag{12}$$

The "$\approx$" sign is because the ensemble average was estimated by the spatial average. Writing out the mean in full

$$\langle L_{\lambda}^{q} \rangle = \int L_{\lambda}^{q} \, \mathrm{d}P(L_{\lambda}) = \int \frac{L_{\lambda}^{q}}{N_{\lambda\,\mathrm{tot}}} \, \mathrm{d}N(L_{\lambda}) = \langle \mathscr{L}_{\lambda}^{q} \rangle \lambda^{-qd} = \lambda^{K_{\mathscr{L}}(q)} \lambda^{-qd} \,. \tag{13}$$

We see that $\tau(q) = (q-1)d - K_{\mathscr{L}}(q)$, so that from $\tau(q)$, we can estimate $D_{\mathscr{L}}(\gamma)$ from $K_{\mathscr{L}}(q)$ using the Legendre transform[11] (Eq. (4)) and $D_{\mathscr{L}}(\gamma) = d - c(\gamma)$.

The most obvious source of bias in this procedure is that it (implicitly) requires unbiased estimates of the probability density $\mathrm{d}P_{\lambda}$, and hence of the unbiased normalization factor $N_{\lambda\,\mathrm{tot}}$ (the total number of galaxies in an unbiased catalogue at resolution λ). Unfortunately, due to the range dependence, not only will the number of dim (low L_{λ}) galaxies be underestimated, but the number missed will depend on λ. This dimension bias or "D bias" for short, yields a biased dimension function $D_b(\gamma)$; it will be

[11] Actually, the dimension formalism of multifractals was used. In addition to the moment scaling exponent $\tau(q)$ discussed above, the dimensions $D(\gamma)$ are denoted as $f(\alpha)$ for a singularity in the integral of L_{λ} order $\alpha = -\gamma$.

explicitly calculated in Section 2.3. To overcome this problem, we construct a series of volume-limited subcatalogues, Section 2.2.

However, there is also a second, more subtle bias, – the "γ bias" which arises from the problem of estimating L_λ in the first place. This is because L_λ is actually the *ratio* between the luminosity at two scales separated by a factor λ; hence any scale-dependent bias in estimating L will shift the orders of singularities by an amount $\gamma_{\rm bias}$. To overcome the γ bias, we use a kind of the bootstrap method which will be described in the next sections.

2. The range-dependent biases of multifractal absolute luminosities

2.1. The effect of the bias

2.1.1. Absolute luminosity singularities

Up until now, we have discussed the properties (including biases) of the GNCs at a general level. We will now be more precise. Consider a catalogue with inner scale r_0, and outer scale R ($R/r_0 = \Lambda$), and denote by L_u the unbiased absolute luminosity. The inner scale is the smallest scale of the cascade (we empirically estimate this below); it is of the order of the typical intergalactic distance. The quantities with subscripts "u" (for "unbiased") are dimensionless ratios of luminosities integrated over the indicated scales

$$L_{u,\Lambda} = \frac{L_{r_0}}{L_{u,R}} = \Lambda^{\gamma_u} \,. \tag{14}$$

The unbiased catalogue scale luminosity $L_{u,R}$ is simply the total luminosity of all the galaxies:

$$L_{u,R} = \sum_{i,\,\rm all} L_{r_0,i} \,, \tag{15}$$

the sum is over all galaxies in the region, including those too dim to detect.

In comparison, the directly empirically accessible luminosities are biased (however, since they are directly measureable, for convenience in the following, the biased quantities will be indicated without special subscripts). Note that at the finest resolution r_0, we typically have a single galaxy, hence if it is detected, there is no bias implying $L_{u,r0} = L_{r0}$. The biased L_Λ is therefore

$$L_\Lambda = \Lambda^\gamma = \frac{L_{r_0}}{L_{u,R}} \frac{L_{u,R}}{L_R} = \Lambda^{r_u} \Lambda^{-\gamma_{\rm bias}} \,, \tag{16}$$

where we have introduced the bias singularity

$$\Lambda^{\gamma_{\rm bias}} = \frac{L_R}{L_{u,R}} \,, \tag{17}$$

with

$$L_R = \sum_{i,\,\rm cat} L_{r_0,i} \,, \tag{18}$$

i.e., the sum is over the (biased) subset of galaxies in the catalogue. In terms of singularities from Eq. (16), we have

$$\gamma_u = \gamma + \gamma_{\text{bias}} . \tag{19}$$

Since the effect of the γ bias is only a shift in the singularities, we can first analyse the observed biased catalogue statistics, use this to estimate γ_{bias} and then make appropriate corrections (shift the γ's); this is the "bootstrap'.

2.1.2. Luminosity density singularities

The luminosity density is given by

$$\mathscr{L}_R = \frac{L_{u,R}}{\text{vol}\, B_R}, \quad \mathscr{L}_{r_0} = \frac{L_{u,r_0}}{\text{vol}\, B_{r_0}} , \tag{20}$$

where "vol" indicates "volume", B_R the "ball" size R; for the catalogues here, it is a region of radius R from the earth subtending a fixed solid angle. Considering only the unbiased luminosity density so that no subscript "u" is used:

$$\mathscr{L}_\Lambda = \frac{\mathscr{L}_{r_0}}{\mathscr{L}_R} = \frac{L_{u,r_0}}{L_{u,R}} \frac{\text{vol}(B_R)}{\text{vol}(B_{r_0})} = \Lambda^{\gamma_{\mathscr{L}}} = \Lambda^{\gamma_u} \Lambda^d . \tag{21}$$

In terms of singularities

$$\gamma_{\mathscr{L}} = \gamma_u + d = \gamma + \gamma_{\text{bias}} + d . \tag{22}$$

2.1.3. Estimating dimension functions using subcatalogues

We have already seen that because of the unknown number of galaxies which are too dim to be detected, the catalogue probability distributions are both D- and γ-biased. The way around the D bias is to use number distributions in a sequence of un-D-biased volume-limited subcatalogues which are un-D-biased for ranges less than $r = \lambda r_0$:

$$N(L_{u,\Lambda}) = p_u(\gamma_u)\lambda^{D_u(\gamma_u)}, \quad L_{u,\Lambda} = \Lambda^{\gamma_u} ,$$

$$N(L_\Lambda) = p(\gamma)\lambda^{D(\gamma)}, \quad L_\Lambda = \Lambda^{\gamma} . \tag{23}$$

Note that although the resolution of the subcatalogues is λ, that of the galaxies remains $\Lambda > \lambda$ (the luminosity is not integrated over a grid, it is always a luminosity of a single galaxy taken from a catalogue with full scale ratio $\Lambda = R/r_0$). Because the volume-limited subcatalogues are un-D-biased (at least for γ's greater than a minimum; see below), we have

$$D(\gamma) = D_u(\gamma_u) = D_{\mathscr{L}}(\gamma_{\mathscr{L}}) . \tag{24}$$

The entire procedure for correcting the biases is therefore to estimate the biased $D(\gamma)$, and then (using the procedure indicated in Section 2.3) find γ_{bias} and then determine $D_u(\gamma_u) = D(\gamma + \gamma_{\text{bias}})$.

2.2. Construction of the subcatalogues

To construct the series of volume-limited subcatalogues, first consider a catalogue with depth R, maximum ratio of scale Λ ($=R/r_0$), and sensitivity (minimum apparent luminosity) $\ell_{\min}$. An important characteristic of the catalogue is the lowest absolute luminosity for which the entire catalogue is unbiased: $R^2\ell_{\min}$. This yields a characteristic luminosity $L_{\Lambda,\mathrm{cat}}$:

$$L_{\Lambda,\mathrm{cat}} = R^2\ell_{\min}/L_R \tag{25}$$

or, in terms of singularities

$$\gamma_{\mathrm{cat}} = \frac{\log L_{\Lambda,\mathrm{cat}}}{\log \Lambda} \tag{26}$$

the entire catalogue is un-D-biased for $L_\Lambda > L_{\Lambda,\mathrm{cat}}$; equivalently for $\gamma > \gamma_{\mathrm{cat}}$.

As with all the formulae below, a convenient way of expressing this is in terms of magnitudes. We therefore introduce the magnitude (M_{mean}) of the catalogue mean absolute luminosity (L_R/N_{cat}):

$$M_{\mathrm{cat}} = -\tfrac{5}{2}\log_{10} L_{\mathrm{cat}}/N_{\mathrm{cat}} + M_{\mathrm{mean}} \tag{27}$$

(recall that 5 magnitudes = factor of 10^2 in luminosity and because of the negative sign, the brightest galaxies have the lowest magnitudes). N_{cat} is the number of galaxies in the catalogue. For reference, various values characteristic of the Z40, CfA2 catalogues are shown in Table 1.

We now construct a series of volume-limited subcatalogues by introducing an absolute luminosity threshold $L_{\Lambda,\min} < L_{\Lambda,\mathrm{cat}}$; these subcatalogues will be un-D-biased for distances up to r given by

$$\begin{aligned} &r = (L_{\Lambda,\min}/\ell_{\min})^{1/2}, \quad L_{\Lambda,\min} < L_{\Lambda,\mathrm{cat}}\,, \\ &r = R, \quad L_{\Lambda,\min} > L_{\Lambda,\mathrm{cat}}\,. \end{aligned} \tag{28}$$

In terms of scale ratios, this corresponds to

$$\begin{aligned} &\lambda = r/r_0, \quad L_{\Lambda,\min} < L_{\Lambda,\mathrm{cat}}\,, \\ &\lambda = \Lambda, \quad L_{\Lambda,\min} > L_{\Lambda,\mathrm{cat}}\,. \end{aligned} \tag{29}$$

Equivalently, the subcatalogues will be unbiased for magnitudes less than

$$\begin{aligned} &M_{\min} = -\tfrac{5}{2}\log_{10} L_{\Lambda,\min}/N_{\mathrm{cat}} + M_{\mathrm{mean}}, \quad M_{\min} > M_{\mathrm{cat}}\,, \\ &M_{\min} = M_{\mathrm{cat}}, \quad M_{\min} < M_{\mathrm{cat}} \end{aligned} \tag{30a}$$

or equivalently, unbiased for singularities greater than

$$\begin{aligned} &\gamma_{\min} = \log L_{\Lambda,\min}/\log \Lambda, \quad \gamma_{\min} < \gamma_{\mathrm{cat}}\,, \\ &\gamma_{\min} = \gamma_{\mathrm{cat}}, \quad \gamma_{\min} > \gamma_{\mathrm{cat}}\,. \end{aligned} \tag{30b}$$

We see that by varying the luminosity/magnitude/singularity threshold defining the subcatalogue, we effectively change the resolution λ of the subcatalogue; however, the

Table 1
Various characteristics of the catalogues. The overall best fit model parameters for the two catalogues are $q_D = 4$, $\gamma_s = -2.25$, $\gamma_c = 2.7$, $\gamma_{\text{bias}} = -0.1$, $\gamma_{\mathscr{L}c} \approx 0.4$, $\gamma_{\mathscr{L}s} \approx 0.85$, $\delta = 0.75$

	Description	Z40	CfA2
Catalogue characteristics			
N_{cat}	Total number of galaxies in the catalogue	1876	1108
$l_{\min}$	Minimum catalogue apparent luminosity	14.5	15.5
R	Maximum depth of catalogue	150 h^{-1} Mpc	150 h^{-1} Mpc
M_{cat}	Lowest magnitude for which the entire catalogue is unbiased	−21.5	−20.5
γ_{cat}	Lowest singularity for which the entire catalogue is unbiased	−2.37	−2.62
M_{mean}	The magnitude of the catalogue mean absolute luminosity	−19.5	−19.1
Fitted model parameters			
r_0	Inner distance of multifractal scaling	13.6 Mpc	17.6 Mpc
Λ	Catalogue scale ratio $= R/r_0$	11	8.5
$D_c = d - C_c$	The dimension of the dim galaxies	1.85	1.85
q_D	Critical exponent of divergence of moments (algebraic tail of the probability distributions)	4.15	3.8
Tail parameters, method 1			
γ_s	Maximum order singularity in a single catalogue	−2.1	−2.2
M_s	Magnitude corresponding to γ_s	−22.3	−21.7
γ_c $(=D_c/q_D - \gamma_s;\ q_D = 4)$	Threshold absolute luminosity singularity for luminosity model	−2.55	−2.65
r_c	Distance corresponding to γ_c	120 h^{-1} Mpc	150 h^{-1} Mpc
M_c	Magnitude corresponding to γ_c	−21.0	−20.5
γ_{bias}	Singularity bias due to the catalogue range dependence	−0.05	−0.01
$\gamma_{\mathscr{L}c}$	Threshold luminosity density singularity for luminosity model	0.5	0.35
$\gamma_{\mathscr{L}s}$	Maximum luminosity density singularity for luminosity model	0.95	0.8
$\delta = C_c - \gamma_{\mathscr{L}c}$	Dark mass exponent	0.65	0.8
Tail parameters, method 2			
γ_s	Maximum order of absolute luminosity singularity in a single catalogue	−2.3	−2.4
M_s	Magnitude corresponding to γ_s	−21.6	−21.3
γ_c $(=D_c/q_D - \gamma_s;$ $q_D = 4)$	Threshold absolute luminosity singularity for luminosity model	−2.75	−2.85
r_c	Distance corresponding to γ_c	95 h^{-1} Mpc	130 h^{-1} Mpc
M_c	Magnitude corresponding to γ_c	−20.5	−20.0
γ_{bias}	Singularity bias due to the catalogue range dependence	−0.1	−0.05
$\gamma_{\mathscr{L}c}$	Threshold luminosity density singularity for luminosity model	0.35	0.2
$\gamma_{\mathscr{L}s}$	Maximum luminosity density singularity for luminosity model	0.8	0.65
$\delta = C_c - \gamma_{\mathscr{L}c}$	Dark mass exponent	0.8	0.95

resolutions of the luminosity values themselves are always at the maximum resolution Λ. In terms of singularities, we can rewrite the subcatalogue resolution as

$$\lambda = \Lambda^{1+(\gamma_{\min}-\gamma_{\text{cat}})/2}, \quad \gamma_{\min} < \gamma_{\text{cat}} ,$$
$$\lambda = \Lambda, \quad \gamma_{\min} \geqslant \gamma_{\text{cat}} \tag{31a}$$

or alternatively

$$\log_{10}\lambda = \log_{10}\Lambda + \tfrac{1}{5}(M_{\text{cat}} - M_{\min}), \quad M_{\min} > M_{\text{cat}} ,$$
$$\lambda = \Lambda, \quad M_{\min} \leqslant M_{\text{cat}} . \tag{31b}$$

We can now express the number count statistics of the un-D-biased volume-limited subcatalogues as

$$N(\gamma) = p(\gamma)\lambda^{D(\gamma)}, \quad \lambda = \Lambda^{1+(\gamma_{\min}-\gamma_{\text{cat}})/2}, \quad \gamma_{\text{cat}} > \gamma > \gamma_{\min} ,$$
$$N(\gamma) = p(\gamma)\Lambda^{D(\gamma)}, \quad \gamma > \gamma_{\text{cat}} ,$$
$$\gamma = \frac{\log L_{\Lambda}}{\log \Lambda} . \tag{32}$$

We can now use the above to test the multifractal hypothesis. For convenience, we rewrite the above in terms of $M_{\min}$, M rather than $\gamma_{\min}$, γ or $L_{\min}$, L:

$$\log_{10} p(\gamma) = \log_{10} N(\gamma) + D(\gamma)\left(\tfrac{1}{5}(M_{\min} - M_{\text{cat}}) - \log_{10}\Lambda\right) ,$$
$$M_{\min} > M_{\text{cat}}, \ \ \gamma_{\text{cat}} > \gamma > \gamma_{\min} , \tag{33a}$$

$$\log_{10} p(\gamma) = \log_{10} N(\gamma) + D(\gamma)\log_{10}\Lambda, \quad M_{\min} < M_{\text{cat}}, \ \ \gamma > \gamma_{\text{cat}} . \tag{33b}$$

In other words, for fixed γ (i.e., luminosity), and $M_{\min} < M_{\text{cat}}$, a graph of $\log N$ vs. $M_{\min}$ will be linear with slope $-D(\gamma)/5$ (this is a variant of the probability distribution/multiple scaling technique used in multifractal analysis [22,23]). An important point to note is that while the subcatalogue (hence N) has the degraded resolution ($\lambda < \Lambda$) the values of the absolute luminosities still have resolution Λ. Since the depth R values of most catalogues are such that only a few bright galaxies are visible at distance R, in practice, few galaxies have $M < M_{\text{cat}}$ so that Eq. (33a) is usually relevant (see below).

2.3. Determining the γ bias

We have seen that by using unbiased subcatalogues, $D(\gamma)$ can be estimated. The final step in correcting the bias is to estimate γ_{bias}, since this is a somewhat involved calculation, this subsection can be skipped at a first reading. We do this by first using the formula for number distribution, to obtain the following biased dimension function $D_b(\gamma)$ (by the method of steepest descents,[12] i.e., by maximizing the exponent over subcatalogues):

$$\Lambda^{D_b(\gamma)} = \int_{\gamma_{\min} < \min(\gamma, \gamma_{\text{cat}})} \Lambda^{(1+(\gamma_{\min}-\gamma_{\text{cat}})/2)D(\gamma)}\, \mathrm{d}\gamma_{\min} . \tag{34}$$

[12] If we ignore prefactors, direct integration can also be used to obtain the same result.

The value of $\gamma_{\min}$ which maximizes the above corresponds to the subcatalogue which dominates the statistics for a given γ. Physically, this determines the largest radius at which the singularity γ can be seen due to the $1/r^2$ fall-off in apparent luminosity. The overall result is

$$D_b(\gamma) = \left(1 + \frac{\gamma - \gamma_{\text{cat}}}{2}\right) D(\gamma), \quad \gamma < \gamma_{\text{cat}} ,$$
$$D(\gamma), \quad \gamma > \gamma_{\text{cat}} . \tag{35}$$

This is presumably the dimension function inferred in Ref. [20].

Now consider the following moment integral:

$$M_q = \int_{\gamma_s > \gamma > \gamma_{\min}} p(\gamma) \lambda^{D(\gamma)} \Lambda^{q\gamma} \, \mathrm{d}\gamma = \int \Lambda^{D_b(\gamma)} \Lambda^{qr} \, \mathrm{d}\gamma . \tag{36a}$$

The corresponding unbiased quantities are

$$M_{q,u} = \int \Lambda^{D_u(\gamma_u)} \Lambda^{q\gamma_u} \, \mathrm{d}\gamma_u . \tag{36b}$$

Using the steepest descents method we can estimate these integrals. Rather than giving the general result which is straightforward but not too illuminating, we give the result for the low-order moments of the threshold model (i.e., $D(\gamma)$ given by Eq. 10). With this thresholded model, we obtain

$$M_q = \Lambda^{(1+(\gamma_c - \gamma_{\text{cat}})/2) D_c + q\gamma_c}, \quad -\frac{D_c}{2} < q < q_D \left(\gamma_c + 1 - \frac{\gamma_s + \gamma_{\text{cat}}}{2}\right) ,$$
$$M_{u,q} = \Lambda^{D_u(\gamma_{u,c}) + q\gamma_{u,c}}, \quad q < q_D . \tag{37}$$

Since the probability is proportional to the number, the above need to be normalized by the total number in the catalogue N_{cat}:

$$N_{\text{cat}} = M_0 = \Lambda^{D_c(1+(\gamma_c - \gamma_{\text{cat}})/2)} . \tag{38}$$

This shows that if the bias is not taken into account, a naive box-counting dimension would yield

$$D_{\text{box}} = \frac{\log N_{\text{cat}}}{\log \Lambda} = D_c(1 + (\gamma_c - \gamma_{\text{cat}})/2) \tag{39}$$

so that (see Table 1) with $D_c \approx 1.85$, $\gamma_c - \gamma_{\text{cat}} \approx -0.1$ to -0.2, we obtain $D_{\text{box}} \approx 1.7$.

Using this estimate of N_{cat}, we obtain

$$\langle L_\Lambda^q \rangle = \frac{M_q}{N_{\text{cat}}} = \frac{M_q}{M_0} \tag{40a}$$

or

$$\langle L_\Lambda^q \rangle = \Lambda^{q\gamma_c}, \quad -\frac{D_c}{2} < q < q_D \left(\gamma_c + 1 - \frac{\gamma_s + \gamma_{\text{cat}}}{2}\right) . \tag{40b}$$

Finally, we obtain the bias

$$\Lambda^{\gamma_{\text{bias}}} = \frac{M_1}{M_{1,u}} = \frac{\Lambda^{D_c(1+(\gamma_c - \gamma_{\text{cat}})/2) + \gamma_c}}{\Lambda^{D_{u,c} + \gamma_{u,c}}} = \Lambda^{(\gamma_c - \gamma_{\text{cat}}) D_c/2 + \gamma_c - \gamma_{u,c}} , \tag{41}$$

where we have used $D_{u,c} = D_c$, and since $\gamma_u = \gamma + \gamma_{\text{bias}}$ we have $\gamma_{u,c} - \gamma_c = \gamma_{\text{bias}}$. Substituting this into the above equation we finally obtain

$$\gamma_{\text{bias}} = (\gamma_c - \gamma_{\text{cat}})D_c/4 \tag{42}$$

so that from Table 1, $\gamma_{\text{bias}} \approx -0.05$ to -0.1 (only slightly different for the two catalogues, depending somewhat on the method of evaluating γ_c).

3. Data analysis

3.1. The data

We have shown that a basic consequence of the multifractal luminosity distribution is that the volume-limited subcatalogues obey Eq. (33). In order to test Eq. (33) we note that it contains both the unknown function $D(\gamma)$ (equivalent to an infinite number of parameters), as well as implicitly the parameter r_0. Even with the restriction of $D(\gamma)$ to the thresholded model, this leaves three parameters $(\gamma_s, \gamma_c, q_D)$ to determine $D(\gamma)$. In addition, the available three-dimensional catalogues (Z40, CfA2) had limited numbers of galaxies, hence simplifying approximations were necessary.

First we briefly describe the catalogues, then the analysis procedure. The three-dimensional position of galaxies is obtained via measurements of their angular position and redshift. In our analysis, all distances are derived from redshift using a Hubble parameter h such that $h = 1$ corresponds to a Hubble constant $H_0 = 100\,\text{km s}^{-1}\,\text{Mpc}^{-1}$ and expansion velocities corrected for virgocentric flow, according to the formula in Ref. [24].

(a) *The Z40 catalogue* is a subsample of the CfA1 catalogue [25] which contains 1876 galaxies in a cone bounded by (in galactocentric coordinates) $b^{II} \geqslant 40^\circ$ and $\delta \geqslant 0^\circ$ with limiting magnitude $l_{\min} = 14.5$ and depth $R = 150\ \text{h}^{-1}\,\text{Mpc}$ (see Fig. 2).

(b) *The CfA2 catalogue* (see Ref. [25]) contains only 1108 galaxies located within a $6^\circ \times 135^\circ$ strip passing through the Coma cluster and has a limiting apparent magnitude $l_{\min} = 15.5$, $R = 150\,\text{h}^{-1}\,\text{Mpc}$); see Table 1 for the basic characteristics (Fig. 3).

(c) *CfA2proj*: This sample is a projection along constant right ascension α of the CfA2 sample. It contains information only on the galaxies' angular position and luminosity and it is therefore treated as a one-dimensional sample (the intersection between a one-dimensional strip and a 2-D projection[13] of the actual 3-D distribution). This is discussed in more detail in Ref. [18], here it is only used to estimate D_c.

(d) *MCG80×80 catalogue*: This sample is a square $80^\circ \times 80^\circ$ centred on the north galactic pole. Its limiting apparent magnitude is 15.5 and contains information on the luminosity and angular position of 6820 galaxies. Since it can be regarded as a two-dimensional projection of the actual 3-D distribution, this sample contains no

[13] It is not quite a full projection since no galaxies further than 150 Mpc are included. However since $D_c < D(\gamma_{\text{cat}})$, this will not affect the statistics here.

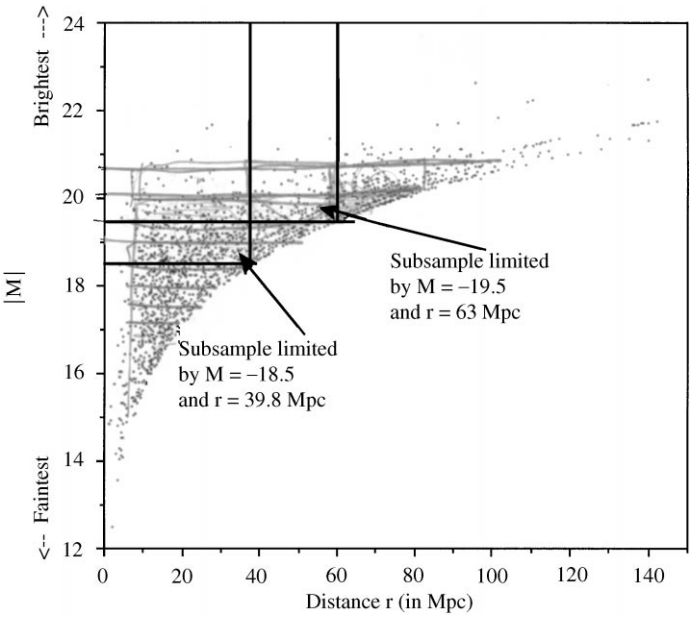

Fig. 2. The radial distribution of the 1876 galaxies in the Z40 catalogue.

information on radial distance. The sample analysed in the next subsection was constructed as follows: from the original data file the angular position of each galaxy (in α and δ) was obtained and then projected onto a plane using a standard equal-area Lambert projection which retains the density of points of the original distribution. A cartesian grid with origin at the north galactic pole was then superimposed onto this plane. Each axis was labeled from -90° to $+90^\circ$ and only those galaxies contained between -40° and $+40^\circ$ (for both axes) were included in the final sample. Note that these were the largest catalogues publicly available at the time the basic analyses were performed; it would be interesting to test the model on larger catalogues such as the Las Campanas survey.

3.2. Estimating D_c

Before testing Eq. (33), we will now outline how various parameters can be directly estimated, showing that they do indeed lead to a $D(\gamma)$ satisfying Eq. (10). First, we estimated the value of D_c in Eq. (10) using the correlation dimension technique. In principle, if $\gamma_c > \gamma_{\text{cat}}$ then $r_c = R$ and $D(\gamma_{\text{cat}}) = D_c$ and so treating the galaxies as a set of points and estimating the dimension will yield D_c. Since the sparseness is constant over the whole catalogue the contribution due to the more intense galaxies (i.e., with $\gamma > \gamma_c$, $D < D_c$) will be negligible (the fractal dimension of any set is the maximum of the dimensions of all its subsets). However, we shall find in both the Z40 and cfA2

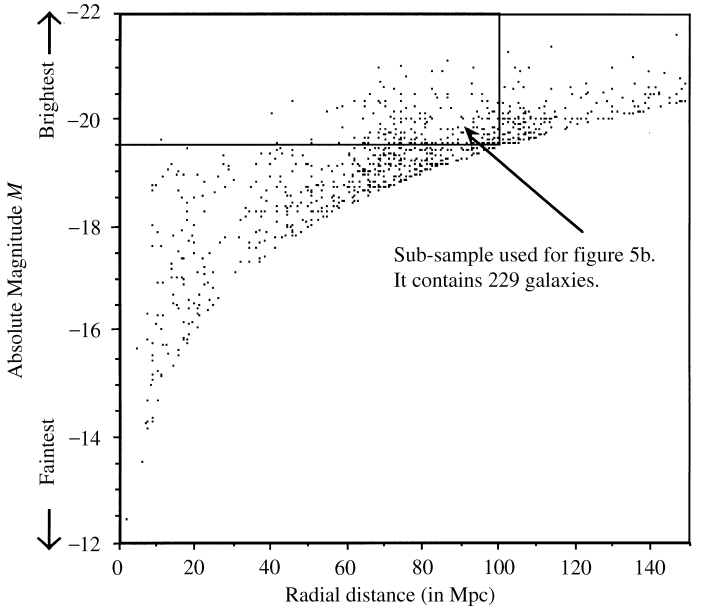

Fig. 3. The CfA2 catalogue of absolute magnitudes M as a function of the distance from the Earth (assuming a Hubble constant of 100 km s^{-1} Mpc^{-1}). As an example, an un-D-biased volume-limited sub-sample with constant threshold was created by selecting those galaxies closer than 100 Mpc and fainter than an absolute magnitude $M = -19.5$. There are 229 such galaxies. In total, there are 1091 galaxies represented in this figure.

catalogues that on the contrary, $\gamma_c < \gamma_{\rm cat}$, $r_c < R$ and $D(\gamma_{\rm cat}) < D_c$. This means that the more distant parts of the catalogue give negligible contributions (it is composed only of extremely sparse bright galaxies). In addition to this dimensional effect, Sylos Labini et al. [2,21] review the considerable literature on scale (i.e., geometric/finite size type) effects, showing that due to the often peculiar geometry of the catalogues (for example the very thin angular slice in the CfA2 catalogue combined with the use of spheres in the standard correlation technique) in conjunction with the range-dependent biases, direct estimates are nontrivial. Indeed, early estimates of D_c were of the order 1.23 [12,26], but larger catalogues and more careful accounting for edge and other effects lead to higher values; Sylos Labini et al. [21] discuss these problems at length and compare many catalogues concluding that $D_c \approx 2 \pm 0.2$ is more accurate.

Although our results are essentially compatible with this (we find $D_c \approx 1.85 \pm 0.05$), it is of interest to consider a slightly different method based on angular projections. As discussed in Ref. [2] angular projections with $D_c < 2$ will have the same D_c, hence since we found $D_c \approx 1.85$, angular projections can be used. Since the catalogues are defined by their angular extent, the angular projections suffer much less from the problems of three-dimensional geometry of the catalogue. Use of the projections has the additional advantage that the much larger apparent luminosity catalogues can be used;

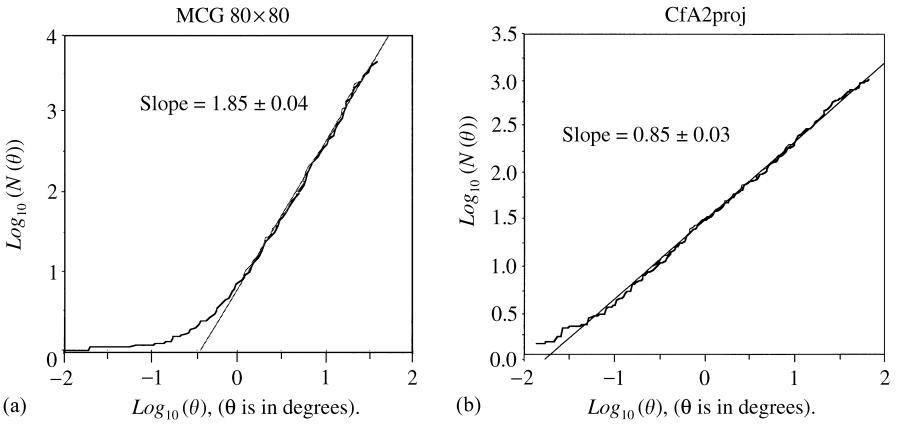

Fig. 4. (a,b) Correlation dimension analysis for the samples MCG80 × 80 and CfA2proj. The values of the corresponding D_c's are obtained from the slopes of the linear region in these figures. The observed values are 1.85 ± 0.04 and 0.85 ± 0.03, respectively, for MCG80 × 80 and CfA2proj, in agreement with the intersection relation. In this figure the quantity θ characterizes the angular box size (in degrees) used in the analysis of these samples.

Fig. 4a shows the result for the M80 with 6842 galaxies, showing $D_c \approx 1.85$. Even for three-dimensional catalogues, projections can make analysis particularly simple, especially when, as for the CfA2 catalogue, it can be treated as nearly an intersection (very thin slice) in one of the angular directions. In this case, we expect the dimension to be reduced by 1 by the intersection; Fig. 4b shows that such a 1-D reprojection of the CFA2 catalogue does indeed yield a 1-D dimension of 0.85 ± 0.03 (up to 100°, i.e., virtually the entire range of angles available) implying $D_c = 1.85$ once again. For comparison, Sylos Labini et al. [2] review the more limited angular correlation analyses and conclude that $D_c \approx 1.8$ with the difference (cf. $D_c \approx 2$) arising from finite size effects and the special nature of the angular projections. For the Z40 catalogue the angular projection was less advantageous; we show below that the same result, $D_c \approx 1.85$, approximately holds by testing Eq. (8) directly. Finally, nearly the same estimate can be obtained by generalizing the "Hubble 3/2 law" to multifractals (Section 4) and then using apparent luminosity histograms. The exponent of the latter (when suitably averaged over the viewing galaxies – see below) yields a direct estimate $D_c/2 \approx 0.93$.

3.3. Estimating γ_s, γ_c, q_D

Contrary to D_c which is determined primarily by the numerous low-brightness galaxies, the parameters γ_s, γ_c, q_D characterize the extreme bright galaxies and – because of their small number – are much more difficult to accurately estimate. We shall see that γ_c and γ_s – the beginning and end of the power-law tail regions – are particularly poorly estimated; indeed it is advantageous to estimate q_D and then use the constraint from Eq. (10b) to obtain $\gamma_c - \gamma_s = D_c/q_D$.

An interesting method of estimating the parameters γ_s, q_D is to use the extremes directly. Combining Eqs. (10b) and (32)

$$N(L) = p(\gamma)\lambda^{q_D(\gamma_s-\gamma)} = p(\gamma)\mathrm{e}^{q_D(\log L_s - \log L)\log\lambda/\log\Lambda}$$
$$= p(\gamma)\left(\frac{L}{L_s}\right)^{-q_L}, \quad \gamma > \gamma_{\min} > \gamma_c\,, \tag{43}$$

$$q_L = q_D\frac{\log\lambda}{\log\Lambda}\,,$$

with $\lambda < \Lambda$ determined by $M_{\min}$ as in Eq. (30) with $M_{\min} < M_{\mathrm{cat}}$. We see that the subcatalogues with $M_{\min} < M_{\mathrm{cat}}$ will give biased exponents $q_L < q_D$ dependent on the subcatalogue via λ. To test this on the Z40, CfA2 catalogues, several volume-limited subcatalogue probability distributions are shown in Figs. 5a and b where we have used the equivalent formulae

$$N(M) = \log_{10} p(\gamma) - \tfrac{2}{5}(M_s - M)q_L\,,$$
$$q_L = \frac{q_D(M_{\mathrm{mean}} - M_{\min})}{5\log_{10}\Lambda}\,, \qquad M > M_{\min},\ M_{\mathrm{cat}} > M_{\min}\,, \tag{44}$$

with M_s being the magnitude corresponding to γ_s. These formulae show that as we vary the subcatalogue (change $M_{\min}$), we obtain straight lines with catalogue-dependent slopes q_L converging at M_s just as indicated in Figs. 5a and b. From these figures, we obtain the estimates $M_s = -22.3, -21.7$ (Z40, CfA2, respectively); we only need estimates of the total scale ratio Λ in order to determine γ_s.

To estimate q_D, Λ, we introduce the easily measurable ratio $\xi = R/r = \Lambda/\lambda$. Hence,

$$q_L = q_D\left(1 - \frac{\log\xi}{\log\Lambda}\right) \tag{45}$$

so that a graph of q_L vs. $\log\xi$ is linear with intercept q_D, and slope $q_D/\log\Lambda$. Note that as $\xi \to 1$, $q_L \to q_D$ as expected. Fig. 6 shows the variation of the slope as a function of $\log\xi$. For both catalogues, the curves display a linear pattern in agreement with Eq. (43), the intercept with $\log\xi = 0$ gives q_D, combined with the slope, we obtain Λ. The straight lines correspond to estimated parameters $q_D = 4.15 \pm 0.15,\ 3.8 \pm 0.15$ for Z40, CfA2 catalogues, respectively. The difference in q_D estimates is not considered too significant; rather, due to poor statistics and also due to the difficulty in accurately determining M_c and hence the region over which the regression to determine q_L is made. We take $q_D \approx 4$ as our best overall estimate. However, the difference in Λ reflects the fact that the two catalogues have different inner scales r_0 (13.6, 17.6 Mpc for Z40, CfA2, respectively) and hence their corresponding Λ's are different: $\Lambda = 11$, 8.5, respectively.

The actual values accessible from the catalogues vary for deep subcatalogues from $q_L \approx 3.9$ down to $q_L \approx 2$ for shallow subcatalogues, the latter being the value cited in Ref. [28]. Because of this relatively low value (e.g. implying a diverging luminosity $q_L = 2$ order moment, i.e., the variance), an exponential cut-off at bright galaxies was introduced in Ref. [28] and the use of cut-offs has become quite popular since; the

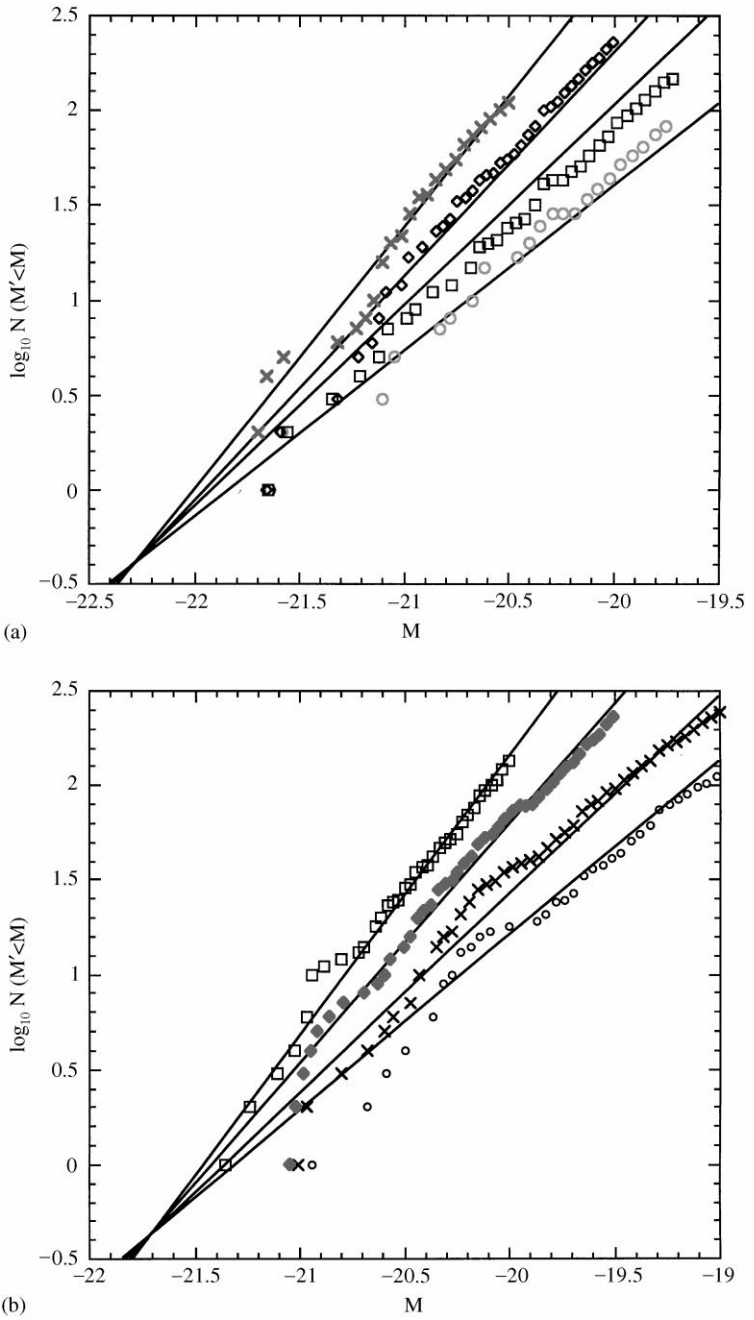

Fig. 5. (a) The histogram of the tails of volume-limited subcatalogues (defined with magnitudes $M_{\min} = -20.5, -20, -19.5, -19$, top to bottom, respectively) for the Z40 catalogue. Lines are fitted with the parameters $\Lambda = 11$, $\gamma_s = -2.09$, $q_D = 4.15$. (b) Same as Fig. 5a except for the CfA2 catalogue (defined with magnitudes $M_{\min} = -20, -19.5, -19, -18.75$, top to bottom, respectively). The straight lines are for the parameters $M_c = -20.5$, $\Lambda = 8.5$, $q_D = 3.8$, $\gamma_s = -2.17$.

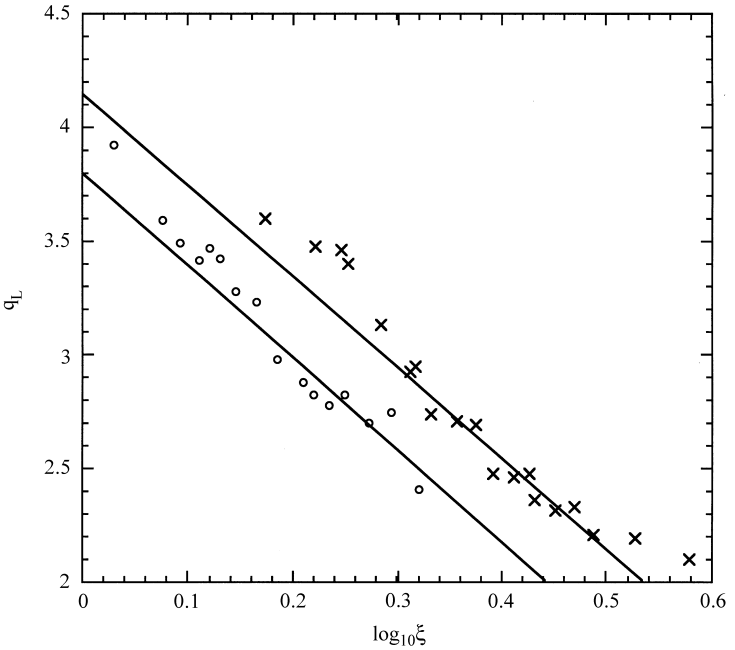

Fig. 6. Variation of the probability exponent q_L as a function of the distance ratio $\xi = (R/r)$; CFA2=open circles, Z40=crosses, reference lines, slope $= -q_D/\log_{10} \Lambda$; $q_D = 3.8, 4.15$, $\Lambda = 8.5, 11$, respectively. Each value of q_L was obtained from a different subcatalogue defined by a specific limiting magnitude $M_{\min}$ and range r. For the two samples CfA2 and Z40 the linearity of the curve fits is compatible with Eq. (7).

critical cut-off magnitude being denoted as M^*. However, our analysis shows that q_L is very sensitive to the Malmquist bias, that the relevant unbiased exponent is ≈ 4, and we no longer need an ad hoc cutoff. It is interesting to note that a survey of estimates of M^* [2] finds values of M^* very close to those of M_c found here (for most catalogues, including CfA2, they report $M^* \approx -19.5$). However, rather than a rapid exponential fall-off (which would contradict the scaling hypothesis), over essentially the same range we find long-tailed algebraic distributions – as generically expected for multifractal processes.

The correspondence between the values of M^* and our M_c is probably better than the above estimates would indicate. This is because M_c is very indirectly estimated: using the equation $\gamma_c = \gamma_s - D_c/q_D$. Even if we consider that D_c, q_D are reasonably accurate, the parameter γ_s is quite poorly estimated so that it is best to consider that the width of the algebraic range ($\gamma_s - \gamma_c = D_c/q_D \approx 0.46$) is fixed, but that the beginning is determined by the magnitude where the multifractal phase transition occurs. On inspection of the probability distributions – see the extent of the linearity in Figs. 5a and b – and in line with the estimates of M^* – we find $M_c \approx -20.5$ and -20.0 for CfA2 and Z40, respectively, corresponding to $\gamma_c \approx -2.75, -2.90$ respectively, and hence $\gamma_s \approx -2.3, -2.4$, respectively. We call this "method 2", see Table 1 for a comparison with the above "method 1". Overall, both catalogues and both methods are

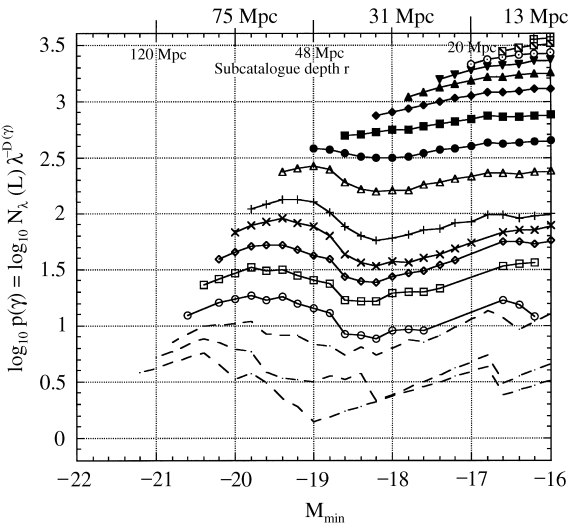

Fig. 7. Above, the $p(\gamma)$ function estimated with Eq. (5); curves bottom to top are for γ's corresponding to $M = -21.4, -21.2, -21.0, -20.8, -20.6, -20.4, -20.2, -20.0, -19.6, -19.2, -18.8, -18.4, -18.0, -17.6, -17.2, -16.8, -16.4$. The bottom three (dashed lines) are those for which $\gamma_{cat} > \gamma > \gamma_c$ ($= -2.09$ here corresponding to, $M_c = -21.0$). Since $M_{cat} = -21.5$, there will be no M_{min} dependence for M less than this (the entire catalogue is unbiased for these very bright galaxies). The multifractality of L is verified by the approximate flatness of the curves. The depth (r) of the subcatalogue is determined by the minimum absolute luminosity (M_{min}) and is found from $r = r_0 10^{(M_{con} - M_{min})/5}$ with $r_0 = R/\Lambda = 150/11 = 13.6$ Mpc. r (on a logarithmic scale) is indicated at the top of the graph.

roughly compatible with the parameters $D_c \approx 1.85$, $q_D \approx 4$, $\gamma_c \approx -2.7$, $\gamma_s \approx -2.25$. Converting to unbiased absolute luminosity density singularities (using $\gamma_{bias} = -0.1$ and Eq. (22)), we have $\gamma_{\mathscr{L}c} \approx 0.4$, $\gamma_{\mathscr{L}s} \approx 0.85$.

3.4. Direct test of $N(\gamma) \approx \lambda^{D(\gamma)}$

Using the above estimates for $D_c, \gamma_c, \gamma_s, q_D, \Lambda$, we can now test Eq. (33) directly by checking the constancy of $p(\gamma)$. Fig. 7 shows the result when this is done for the Z40 catalogue. The relative flatness of the estimates of $p(\gamma)$ as M_{min} (and hence the scale ratio λ) is varied for fixed M (i.e., γ) confirms that the parameter estimates are reasonable.

4. The multifractal Hubble 3/2 law: how apparent luminosity distributions can be explained by multifractality

4.1. The relation between absolute and apparent luminosity distributions

Garrido et al. [18] did not attempt to resolve the range-dependent bias problems discussed above; rather, the view was taken that the apparent luminosities were relatively

well estimated, and that scale invariance should imply that they are also multiscaling, a prediction empirically verified on the M80 and the 1-D projection of the CfA2 catalogues. However, we can now return to the problem of interpreting the apparent luminosities taking into account (a) the large statistical fluctuations (emphasized in Ref. [21], and (b) the theoretical connection between multifractal absolute luminosities obtained by generalizing Hubble's "3/2" law for apparent luminosities.

We first recall the classical derivation of the Hubble 3/2 law [29]. Consider a catalogue limited by a constant apparent luminosity ℓ (apparent magnitude $\bar{m}$). Suppose first that all galaxies in the catalogue have the same absolute luminosity L. Then, the number of galaxies with apparent luminosity greater than $\ell(N(l'>l))$ equals the number of galaxies which are closer than $r \sim \sqrt{L/\ell}$. For galaxies distributed with a dimension D, this implies that $N(\ell' > \ell) \sim r^D \sim (L/\ell)^{D/2}$ (Hubble took $D=3$). Since not all galaxies have the same absolute luminosity L, we can generalize this result by integrating over all L values:

$$N(\ell' > \ell) \propto \int \left(\frac{L}{\ell}\right)^{D/2} \mathrm{d}L \propto \ell^{-D/2} = \ell^{-q_\ell} ,$$
$$q_\ell = D/2 , \tag{46}$$

where q_ℓ is the apparent luminosity exponent. At the Earth, the observed value of q_ℓ is ≈ 1.35 [18,21]; significantly larger than the value $\approx 0.93 - 1$ predicted by using the monofractal model with D_c in the range 1.85–2. Sylos Labini et al. [21] have argued that in spite of this discrepancy the monofractal picture is nevertheless correct and that the discrepancy is due to local bias. They demonstrate this by averaging over all the galaxies (using a kind of double volume-limited statistic), a procedure we follow below and which indeed yields $q_\ell \approx 0.93$ (although – due to multifractality – not over the whole range of ℓ; see below).

Now consider a multifractal absolute luminosity distribution. We define the apparent luminosity (analogue) dimension function and singularity γ_ℓ:

$$N(L' > L) \propto \Lambda^{D(\gamma)}, \quad L = \Lambda^{\gamma} ,$$
$$N(\ell' > \ell) \propto \Lambda^{D_\ell(\gamma_\ell)}, \quad \ell = \Lambda^{\gamma_\ell} . \tag{47}$$

Extending the monofractal Hubble law to the multifractal case, we obtain

$$N(\ell' > \ell) \approx \Lambda^{D_\ell(\gamma_\ell)} \sim \int \Lambda^{(\gamma-\gamma_\ell)D(\gamma)/2} \, \mathrm{d}\gamma . \tag{48}$$

Now, rather than integrate over singularities, we can consider γ as a function of D, and integrate over dimensions

$$N(\ell' > \ell) \approx \int \Lambda^{D\gamma(D)/2-\gamma_\ell D/2} \, \mathrm{d}D . \tag{49}$$

This expression shows that $N(\ell' > \ell)$ is the Laplace transform of $\Lambda^{D\gamma(D)/2}$, and hence $N(L)$ can be obtained from $N(\ell' > \ell)$ by the inverse Laplace transform. The Laplace transform pair $\Lambda^{D\gamma(D)/2}$, $\Lambda^{D_\ell(\gamma_\ell)}$ is analogous to the multifractal probability-moment pair: $\Lambda^{c(\gamma)}$, $\Lambda^{K(q)}$ (see Eq. (4)) introduced earlier. In the case of large L, it also reduces (via

the method of steepest descents) to a Legendre transform pair for the exponents

$$2D_\ell(\gamma_\ell) = \max_{-D} [(-D)\gamma_\ell - (-D\gamma)] , \tag{50a}$$

$$-D(\gamma)\gamma = \max_{\gamma_\ell} [(-D)\gamma_\ell - 2D_\ell(\gamma_\ell)] . \tag{50b}$$

The values of D and γ_ℓ where the maximum occurs provide one-to-one relations between D (and hence γ) and D_ℓ (and hence γ_ℓ). The first (Eq. (50a)) yields

$$\gamma_\ell = \frac{D(\gamma)}{D'(\gamma)} + \gamma \tag{51}$$

which is the relation between γ_ℓ and γ showing that it is one to one except over ranges where $D(\gamma) =$ constant. Differentiating this and using the fact that $D'' < 0$ ($D(\gamma)$ is concave) and $D' < 0$ ($D(\gamma)$ is monotonically decreasing), $D > 0$ shows that $\mathrm{d}\gamma_\ell/\mathrm{d}\gamma > 0$, i.e., we find that γ_ℓ is an increasing function of γ.

The second maximization (Eq. (50b)) leads to a particularly simple relation

$$D'_\ell(\gamma_\ell) = -D(\gamma)/2 , \tag{52}$$

i.e., the absolute logarithmic derivative of $N(\ell' > \ell)$ is half the fractal dimension of the contributing set. In order to obtain an even simpler expression, consider the q_ℓ moments of ℓ:

$$\langle \ell^{q_\ell} \rangle = \Lambda^{K_\ell(q_\ell)} = \int \Lambda^{\gamma_\ell q_\ell - (d - D_\ell(\gamma_\ell))} \, \mathrm{d}\gamma_\ell, \quad d = 3 . \tag{53}$$

Once again, we obtain Legendre transform relations between $c_\ell(\gamma_\ell) = d - D(\gamma_\ell)$ and $K_\ell(q_\ell)$. The first of these leads to the standard multifractal relation between statistical moments order q_ℓ and the singularity (and dimension) dominating the moment

$$q_\ell(\gamma_\ell) = -D'_\ell(\gamma_\ell) , \tag{54}$$

i.e., q_ℓ is the (negative) logarithmic derivative of N. Hence, combining this with the above relation between D and D_ℓ, we obtain the following generalization of the Hubble 3/2 law:

$$q_\ell(\gamma_\ell) = D(\gamma)/2 . \tag{55}$$

This generalizes the nonfractal ($D = 3$) or monofractal case (D is constant < 3), which would imply that D_ℓ is linear (Eq. (52); $D_\ell = q_\ell\gamma_\ell$) as expected. However, in the more general multifractal case, D is variable, leading to nonlinear D_ℓ. A general property of dimension functions $D(\gamma)$ is that they are decreasing concave functions; however, by differentiating Eq. (52) and using the fact that $D' < 0$, $\mathrm{d}\gamma_\ell/\mathrm{d}\gamma > 0$ we can easily show that D_ℓ is convex; it is not a true dimension function. This is perhaps not too surprising since the apparent luminosities are angular projections; a given angular separation involves galaxies with widely varying spatial distances. The relationship

between the angular multifractal dimensions in Ref. [18] and (fine scale) luminosity exponent $D_\ell(\gamma_\ell)$ is not known at present.

4.2. The multifractal Hubble 3/2 law with the threshold model for $D(\gamma)$

We have argued that the actual $D(\gamma)$ for the absolute luminosities can be reasonably approximated by the model equation (10) with the parameters given in Table 1. Before comparing the model to the empirical apparent luminosity data we will first give the corresponding exponent $D_\ell(\gamma_\ell)$ in this special case. The simplest way to obtain the relationship is to first consider the algebraic tail; $\gamma_s > \gamma > \gamma_c$. According to the Legendre transform above, we find the following relation between singularities:

$$\gamma_\ell = 2\gamma - \gamma_s, \quad \gamma_s > \gamma_\ell > \gamma_{\ell c} \tag{56a}$$

with

$$\gamma_{\ell c} = 2\gamma_c - \gamma_s \tag{56b}$$

being the lower bound on the nonlinear part of the apparent luminosity dimension function. For the regime in which the dimension $D(\gamma) = D_c = \text{constant}$, we obtain a linear D_ℓ; Eq. (52) shows that $D'_\ell = -D_c/2 = \text{constant}$ in this regime. Overall, we obtain

$$D_\ell(\gamma_\ell) = \frac{q_D}{8}(\gamma_s + \gamma_{\ell c} - 2\gamma_\ell)(\gamma_s - \gamma_{\ell c}), \quad \gamma_\ell < \gamma_{\ell c}\,,$$

$$D_\ell(\gamma_\ell) = \frac{q_D}{8}(\gamma_s - \gamma_\ell)^2, \quad \gamma_s > \gamma_\ell > \gamma_{\ell c}\,. \tag{57}$$

The width of the nonlinear regime, is thus $\gamma_s - \gamma_{\ell c} = 2(\gamma_s - \gamma_c) = 2D_c/q_D \approx 0.9$ which is fairly narrow. As we see in the next section, this combined with the large fluctuations at the tail end – probably explains why it has not been noticed up until now.

4.3. Empirical test of the multifractal Hubble 3/2 law

In order to empirically test the above and to use the absolute luminosities to predict the apparent luminosity distribution – we note that due to the expected extreme variability of the multifractal cascade, we anticipate strong statistical variations as mentioned above. In order to obtain robust estimates, we therefore follow Ref. [21] by determining the average apparent luminosity exponent over all the available galaxies by averaging over all (galaxy centred) viewing locations using a kind of "double volume-limited catalogue" to avoid bias. The result of this analysis is shown in Fig. 8. In this figure we show the averaged GNCs for both the Z40 and the CfA2 catalogues, as well as the corresponding GNCs computed as seen from the Earth only. Two clear features can be observed. First, it is clear that for galaxies brighter than $m = 15.5$, the GNCs display roughly a power-law behaviour with an exponent $2/5q_\ell \approx 0.37 \pm 0.02$, hence $D'_\ell \approx 2q_\ell = 1.86 \pm 0.08$, i.e., nearly identical to $D_c \approx 1.85$. Notice that this value is also smaller than the slope predicted by the GNC seen from the Earth only. Since our

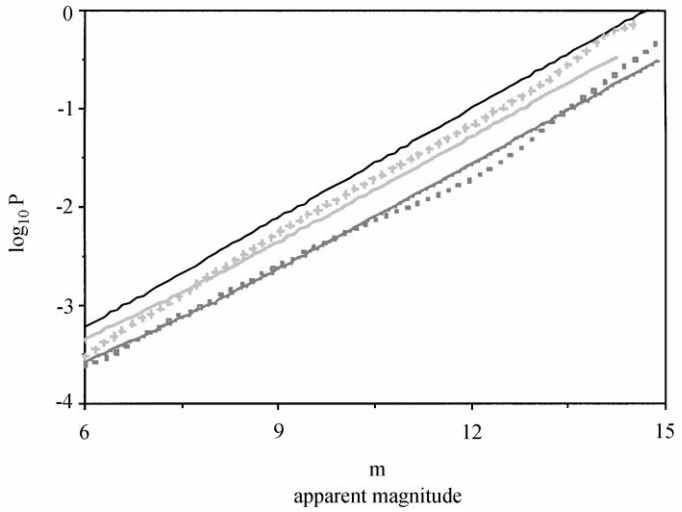

Fig. 8. At the top is the reference line $\log_{10} P = 0.37m - 5.45$ (corresponding to monofractal with $D_c = 1.85$), the curved lines are simulations with $q_D = 4.15$, $\gamma_s = -2.25$, $D(\gamma) = D_c = 1.85$ for $\gamma < \gamma_D$, $D(\gamma) = (\gamma_s - \gamma)q_D$ for $\gamma > \gamma_D$. Points are corresponding data curves averaged in the "double" volume-limited way described in the text (top is CfA2, bottom, Z40).

estimate of 1.86 arises from the ensemble average of the 1108 galaxies of the CfA2 catalogue and the 1876 galaxies of the Z40 catalogue, it is clear that it is more statistically significant than the estimates done solely from the Earth. The relatively high value of the estimate obtained from the Earth can be justified as an ordinary statistical fluctuation from the spatial ensemble average (an estimate of q_ℓ can be made using each galaxy as a centre, the resulting distribution of q_ℓ for all the different galaxies has a large standard deviation $\approx \pm 0.6$ so that the Earth-based estimate is within a single standard deviation of the ensemble estimate).

In order to account for both the nonextreme ($D(\gamma) = D_c = 1.85 = \text{constant}$) and extreme (linear $D(\gamma)$) behaviour, it is enough to consider the simple model for the absolute luminosities discussed above with the parameters $D_c = 1.85$, $q_D = 4$, $\gamma_s = -2.25$, and $\gamma_c = -2.7$. Fig. 8 shows the comparison with the apparent luminosity data obtained by using the corresponding $D_{(\gamma)}$ function in Eq. (48). As can be seen, the agreement for both catalogues is very good, especially given the relatively small number of galaxies involved and the simple model for $D(\gamma)$. The nonlinearity associated with $\gamma > \gamma_c$ is slight; analysis shows that the corresponding $\gamma\ell$ values are in the interval $\gamma_{\ell c} < \gamma_\ell < \gamma_s$ with $\gamma_{\ell c} = -\gamma_s + 2\gamma_c \approx -3.15$. Hence with $\Lambda \approx 10$ this corresponds to the range of magnitudes of $0.9 \times 2.5 \approx 2.2$ at the extreme (left) side of Fig. 8). However, as Fig. 8 shows, for the actual (relatively small) Λ's used here, the actual apparent luminosity probabilities (proportional to N) are only slightly nonlinear; a clear discontinuity at γ_c will only be visible for large Λ.

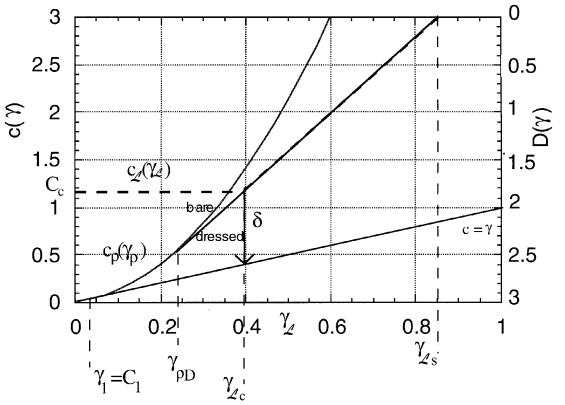

Fig. 9. Schematic with hypothetical mass density codimension function (subscript "ρ"; solid line, using the universal multifractal model parameters $C_1 = 0.033$, $\alpha = 2$; the bare c_ρ is curved, the dressed c_ρ is linear for $\gamma > \gamma_{\rho D}$) with multifractal phase transition at $\gamma_{\rho D} = 0.23$ for divergence of moments of order $q_D = 4$ (shown as an asymptote). The luminosity density codimension $c_{\mathscr{L}}(\gamma_{\mathscr{L}})$ is indicated by heavy dashed lines with threshold at $\gamma_{\mathscr{L}c} = 0.4$, and the corresponding dimension $D_c = 1.85$. The dark mass exponent δ is shown graphically (here ≈ 0.75). $\gamma_{\mathscr{L}s} \approx 0.85$ is the maximum observed order of singularity.

5. Implications for dark matter and Hubble law

5.1. Dark matter

Turning our attention to the unbiased model for $\mathscr{L}$, we have argued that in order to account for both the nonextreme ($D_{\mathscr{L}}(\gamma_{\mathscr{L}}) = D_c = 1.85 = \text{constant}$) and extreme (linear $D_{\mathscr{L}}(\gamma_{\mathscr{L}})$) behaviour, it is enough to consider a simple thresholded model for the absolute luminosities with the parameters given in Table 1. Physically, it is quite easy to see how such a thresholded $D_{\mathscr{L}}(\gamma_{\mathscr{L}})$ could arise. Consider the (convex) codimension function $c_{\mathscr{L}}(\gamma_{\mathscr{L}}) = d - D_{\mathscr{L}}(\gamma_{\mathscr{L}})$ which is the exponent for the probability distribution (see Fig. 9). First, consider the "bare" codimension function for the mass density; this is the direct result of a cascade process hierarchically concentrating mass down to subgalactic (nonobserved) scales. The observed "dressed" codimension function will be the overall result integrated over the larger galactic scale. As mentioned earlier, this generically produces (via a first-order multifractal phase transition at $\gamma_{\mathscr{L}} = \gamma_{\mathscr{L}D}$ [8,9]), the power-law tail (corresponding to self-organized critical behaviour) indicated by the straight-line asymptote in Fig. 9. Similarly, constant, nonextreme behaviour for $\gamma_{\mathscr{L}} < \gamma_{\mathscr{L}c}$ generically arises via a simple thresholding effect at the smallest scale followed by an integration (dressing) to the observed scale Λ [10]. Such a "monofractal filter" would correspond to the existence of a minimum threshold for luminous mass concentrations. Above the threshold, mass and luminosity could be roughly linearly related (Eq. (6)), below the threshold the mass would be "missing" in the sense that it would be in nonluminous concentrations. We now show that it is also compatible with estimates of the mass of dark matter.

5.1.1. Direct estimate of dark matter

Let us suppose that the total scale ratio of the mass cascade is Λ'; we have seen that if the outer scale is 1000 h^{-1} Mpc [2], then this may be of the order of 10^2; our $150\,h^{-1}$ Mpc deep catalogues already spanned the range $\Lambda \approx 10$; this is already nearly the maximum compatible with the standard model; see Fig. 1. Consider the implications of this simple model for luminosity-based estimates of the mass of the universe. Assuming that the mean density is scale independent (conserved by the cascade; $\langle \rho_\Lambda \rangle = 1$), we find $\langle \mathscr{L}_\Lambda \rangle = \Lambda^{-\delta}$ where δ is given by

$$\delta = \min_{\gamma}(c(\gamma) - \gamma) = C_c - \gamma_c = (d - D_c) - \gamma_c \tag{58}$$

(Eq. (4) for $q = 1$; see Fig. 9); this yields the estimate $\delta \approx 0.75$ (Table 1).

This extra mass is "missing" from the standard (homogeneous, $\delta = 0$) estimates; δ is a "dark mass exponent". For example, taking the estimates $\Lambda' = 100$, 10, we obtain the factors $(100)^{0.75} \approx 30$, $(10)^{0.75} \approx 6$; the visible mass is thus respectively $\approx 3\%$, 15% of the total. According to a survey by Peebles [7], current estimates place the density of luminous matter in "rich clusters" of galaxies at $\Omega = 0.01$, this would imply that the total density (baryonic and nonbaryonic) is, respectively, $\Omega \approx 0.3$, 0.06, the former of which is in line with the latest estimates from redshift–distance relations from supernovae [30].

5.1.2. Indirect estimate of dark matter

Even over the narrower range of scales spanned by the catalogues considered here ($\Lambda \approx 10$), there will be a factor $10^{0.75} \approx 6$ ratio of dark to luminous matter. This is roughly compatible with ratios determined by large-scale dynamics (obtained by considering their peculiar velocities within clusters and which includes estimates of dark matter directly associated with galaxies), which Peebles places in the range $0.05 < \Omega < 0.1$. Note that according to our model, we expect the results of such studies to yield progressively larger density estimates until the true outer scale ratio Λ' is reached.

5.2. The de Vaucouleurs–Hubble "paradox"

The primary criticism of scaling models of the large-scale structure of the universe is that they involve unacceptably large fluctuations in mean density. For example, the COBE temperature fluctuations are believed to be proportional to fluctuations in the gravitational potential (and hence indirectly proportional to the density) at the epoch of radiation/matter decoupling; it is argued that they are small enough to preclude a large outer scale for the scaling (see Fig. 1). Similarly, in the standard big bang expansion model, the Hubble law follows if the density is uniform, hence the fact that it is accurately followed even for distances of only several Mpc (see Ref. [2]) implies that the fluctuations in mean density are small.

Let us therefore consider the fluctuations in the mean in the multifractal model. First, the Legendre relation (Eq. (4)) establishes a one-to-one correspondence between statistical moments and singularities. In particular, the mean ($q = 1$ order moment) whose

corresponding singularity value is denoted as $\gamma_1 = K'(1)$ has corresponding codimension $c(\gamma_1)$ denoted as C_1. Therefore, if C_1 is small enough (the corresponding $D_1 = d - C_1$ is close enough to $d = 3$), the density fluctuations giving the dominant contribution to the mean will be nearly uniform ($c = 0$) – even though those associated with luminous matter are very sparse ($C_c \gg C_1 \approx 0$). Although we have no direct information on the form of $c_\rho(\gamma_\rho)$ for $\gamma_\rho < \gamma_{\mathscr{L}c}$ (and hence on the value C_1), our parameter estimates severely limit the possible range. To see this, consider the equations satisfied by the multifractal phase transition

$$(d - c_\rho(\gamma_{\rho D})) = q_D(\gamma_s - \gamma_{\rho D}), \quad \gamma_{\rho D} = K'_\rho(q_D)\,. \tag{59}$$

The first equation simply states that for $\gamma_\rho > \gamma_{\rho D}$ (where the first-order multifractal phase transition occurs) c_ρ becomes linear passing through the point $c_\rho(\gamma_s) = d$. The second is simply the Legendre relation between the critical singularity ($\gamma_{\rho D}$) and the corresponding moment (q_D). As long as Eq. (59) is satisfied with $\gamma_{\rho D} < \gamma_{\mathscr{L}c}$, the model will be consistent with the observations. Substituting the Legendre relation $K_\rho(q_D) = q_D\gamma_{\rho D} - c_\rho(\gamma_{\rho D})$ into Eq. (59), we obtain

$$K_\rho(q_D) = q_D\gamma_s - d\,. \tag{60}$$

Before substituting the empirical values on the right-hand side, we may already note that since $q_D > 1$, we have $K_\rho(q_D) > 0$ which implies the constraint $\gamma_s > d/q_D \approx 3/4$. Substituting in the parameters estimated earlier, we find the constraint $K_\rho(4) = 4 \times 0.85 - 3 = 0.4$. To show that this value is readily compatible with small values of C_1, consider the hypothesis that the cascade dynamics leads to universal multifractal mass densities:

$$K_\rho(q) = \frac{C_1}{\alpha - 1}(q^\alpha - q), \quad q < q_D\,, \tag{61}$$

where $0 \leqslant \alpha \leqslant 2$ is the Levy index which parametrizes the degree of multifractality, empirically, $q_D \approx 4$ (Table 1). The extreme case $\alpha = 2$, corresponds to the "log-normal" multifractal and $\alpha = 0$ to the monofractal ("beta model") limit. Over the entire range of possible α values, the constraint $K_\rho(4) = 0.4$ limits C_1 to the range 0.03 ($\alpha = 2$) to 0.13 ($\alpha = 0$) with corresponding $\gamma_{\rho D}$ in the range 0.23–0.13, i.e., $< \gamma_{\mathscr{L}c}$ for all values of α (cf. the empirical value $\gamma_{\mathscr{L}c} \approx 0.4$, Table 1). In particular, for $\alpha = 2$, the corresponding dimension $D_1 \approx 3 - 0.03 \approx 2.97$ is sufficiently close to 3 so that for example even if $\Lambda' = 100$, then the variations in the density levels relevant to the mean are small. To make a quantitative estimate, we can follow Sylos Labini et al. [2] and use the linear perturbation theory to relate the relative peculiar velocity $\delta V/V_H$ (V_H is the Hubble velocity) to the relative density fluctuations $\delta\rho/\rho$ obtaining

$$\delta V/V_H = -\tfrac{1}{3}\Omega^{0.6}\delta\rho/\rho\,. \tag{62}$$

If we now take $\delta\rho$ as the standard deviation, for our multifractal model we obtain

$$\delta\rho/\rho = (\Lambda^{K_\rho(2)} - 1)^{1/2}\,. \tag{63}$$

Taking $K_\rho(2) = 0.066$ ($C_1 = 0.033$, $\alpha = 2$), and $\Lambda = 100$, 10 we obtain $\delta\rho/\rho \approx 60\%$, 40%, respectively, for the relative density fluctuation at the inner cascade scale

(≈ 10–$15\ h^{-1}$ Mpc). Finally, taking $\Omega \approx 0.3$, we obtain $\delta V/V_H \approx 5$–10%, 3–7% ($\Lambda =$ 100, 10, respectively) which is compatible with the observed fluctuations in the Hubble law (which are probably of the order of 10% at $60\ h^{-1}$ Mpc).

5.3. Mass and luminosity spectra

The basic element of our model is the assumption that the luminous matter is only the extreme end of a hierarchy of density singularities. We have seen that this is probably sufficient to reconcile the scaling with the fluctuations in the Hubble law. It also predicts that the spectra for luminous matter and density are quite different. As a final aid in comparing our model with the standard big bang models, we now estimate the exponents of the standard power spectral density ($P(k)$):

$$P(k) \approx k^{-s} . \tag{64}$$

Since the spectrum is the Fourier transform of the autocorrelation (a second-order statistic), for a multifractal embedded in an isotropic d-dimensional space, we obtain the standard result (e.g. Ref. [27])

$$s = d - K(2) - 2K(1) , \tag{65}$$

where $K(2)$ is the value of the scaling moment exponent for $q = 2$. Applying this to our lognormal model of density and the thresholded model of luminosity, we obtain, respectively

$$s_\rho = d - 2C_1, \quad s_{\mathscr{L}} = d - C_c . \tag{66}$$

Using the values $d = 3$, $C_1 = 0.033$, $C_c = 1.15$, we obtain $s_\rho = 2.93$, $s_{\mathscr{L}} = 1.85$. These lines – adjusted so that the outer scale is at $150\ h^{-1}$ Mpc – the outer scale of this study – are indicated in Fig. 1. We see that as expected, the line corresponding to the luminosity spectrum goes quite accurately through the galaxy data points, but that the spectral density at scales of $10\ h^{-1}$ Mpc is already overestimated by a factor of ≈ 10 due to the assumption that matter is tracked by luminosity.

6. Conclusions

We gave argued that the generic result of scaling nonlinear cascade dynamics is multifractal galaxy number counts with nonfractal and monofractal models as special cases. The main problem in verifying this simple prediction is the existence of large range-dependent biases; both in the dimensions (the "D bias") and (to a much lesser degree) in the singularities (the "γ bias"). The D bias can be removed by systematically applying an extension of a basic multifractal ("PDMS") analysis technique to volume-limited subcatalogues, while the γ bias is simply a shift in singularities and can be removed by a kind of bootstrap procedure in which the un-D-biased number distributions can be used to estimate the γ bias. Removing these biases, we demonstrated the multifractality for the Z40 and CfA2 catalogues (including the extremes). The multifractality was shown to be compatible with a simple "thresholded" model in

which the dimension is constant up until a critical singularity (a multifractal phase transition) after which the dimension function becomes linear corresponding to algebraic probabilities, "self-organized critical behaviour". A qualitative change in behaviour at nearly the same galaxy magnitudes was also noted in the literature but was on the contrary attributed to exponential (nonscaling) behaviour of the extremes.

The parameters of the thresholded model were estimated by using angular projections, as well as by using apparent luminosities. In order to infer the model parameters from the latter, we showed how to extend the Hubble 3/2 law (relating absolute and apparent luminosities) to multifractal absolute luminosity distributions showing that, in general, the logarithmic derivative of the apparent luminosity distribution (when suitably averaged using double volume-limited catalogues), is half the fractal dimension of the corresponding absolute luminosity.

We then suggested a simple model which would explain the observed $D(\gamma)$ function. In our model, a cascading hierarchy of mass density flux starts at large scales (perhaps as much as 1000 h^{-1} Mpc or larger) and proceeds via a scale-invariant series of instabilities down to the mean intergalactic distance (or smaller). This generically produces a multifractal mass density distribution, including (via first-order multifractal phase transitions), algebraic tails on probability distributions (we find a critical exponent $q_D \approx 4$ corresponding to the divergence of moments of order 4 and higher) associated with extreme mass concentrations – self-organized critical structures. However, in the model the luminosity density only "tracks" the mass density for singularities greater than a critical value corresponding to a minimum threshold for galaxy formation. Lower-order mass density singularities (below $\gamma \approx 0.4$) are nonluminous. Since the mass clusters/singularities giving the dominant contribution to the mean mass are below the threshold, we conclude that most of the mass in the universe is in dark clusters. Extrapolating from locally calibrated luminosity – mass relationships to scales much larger than the calibration catalogue, we require a "missing mass" exponent which we estimate to be $\delta \approx 0.75$. This value is sufficiently high so that for example if the cascade starts at 1000 h^{-1} Mpc (about 7 times the scale of our catalogues), then 97% of the mass is dark; with this large outer scale, we predict $\Omega \approx 0.3$ which is the currently favoured value.

In addition to a simple accounting for missing mass – whether baryonic or nonbaryonic – our model also resolves the apparent contradiction between the excellent (but nontrivial (multi)fractal) scaling of the luminous mass (suggested by de Vaucouleurs, quantified by the minimum codimension $C_c \approx 1.15$), and the equally impressive linearity of the Hubble law (even at small scales). Since it is hard to renconcile a highly heterogeneous distribution of mass with a linear Hubble law, Sylos Labini et al. [2] call this the "de Vaucouleurs–Hubble" paradox. However, in our model – at least as concerns the low-order statistics including the mean and variance – the heterogeneity of the mass is much less than that of the luminosity: (e.g. for the lognormal model, $D_1 = 2.97$ compared to $\max(D) = 1.85$ for the luminosity density), using the linear perturbation theory, we estimate that velocity fluctuations around the Hubble law at 10–15 h^{-1} Mpc will be in the range 3–10%.

Our knowledge of the large-scale density fluctuations of the universe comes essentially from measurements of the microwave background interpreted with the help of various cosmological models, and from measurements of the luminosity interpreted with the help of assumptions relating luminosity to mass. In the last 10 years as measurements of all kinds have improved, we have witnessed an apparent contradiction between the largest scale of heterogeneity of galaxy catalogues which has been progressively pushed further out, while simultaneously, the smallest scale of density homogeneity scale as inferred from the microwave background, has been more confidentaly pushed inwards. The model presented here shows how – if the cross-over scale occurs somewhere near 150 h^{-1} Mpc – the two can be reconciled. This model could be viewed as a kind of compromise between the two empirical findings since it allows the component of the mass density field giving the dominant contribution to the mean to be relatively spatially homogeneous while allowing the much denser luminous component to be highly heterogeneous/sparse with the two tied together with the simple hypothesis that only sufficiently dense regions are luminous. Future work to test this model could benefit, on the one hand, from the use of much larger galaxy catalogues, and on the other hand, from the results of N-body calculations which may already have a sufficient range of scales to estimate the parameters.

Acknowledgements

We acknowledge useful discussions with M. Montuori, P.J.E. Peebles and M. Geller. We particularly acknowledge long discussions with M. Hudson who made helpful suggestions about reconciling the cosmological models with the scaling observations and who suggested various pertinent references.

References

[1] D. Schertzer, S. Lovejoy, F. Schmitt, Y. Chigirinskaya, D. Marsan, Fractals 5 (1997) 427–471.
[2] F. Sylos Labini, F. Montuori, L. Pietronero, Phys. Rep. 293 (1998) 61–226.
[3] E. Gawiser, J. Silk, Science 280 (1998) 1405.
[4] S. Lovejoy, D. Schertzer, Can. J. Phys. 46 (1990) 62.
[5] D. Schertzer, S. Lovejoy, Physico-Chem. Hydrodyn. J. 6 (1985) 623–635.
[6] D. Schertzer, S. Lovejoy, J. Geophys. Res. 92 (1987) 9693–9714.
[7] P.J.E. Peebles, Principles of Physical Cosmology, Princeton University Press, Princeton, NJ, 1994.
[8] D. Schertzer, S. Lovejoy, in: M.M. Novak (Ed.), Fractals in the Natural and Applied Sciences, Elsevier, North-Holland, 1994, pp. 325–339.
[9] D. Schertzer, S. Lovejoy, Phys. Rep. 2000, in press.
[10] C. Larnder, M.Sc. Thesis, McGill, 1995.
[11] C.V.L. Charlier, Arkiv. förMat. Astron. Fys. 4 (1908) 1.
[12] d. Vaucouleurs, Science 167 (1970) 1203.
[13] B.B. Mandelbrot, C.R. Acad. Sci (Paris) A 280 (1975) 1551.
[14] P.H. Coleman, L. Pietronero, Phys. Rep. 213 (1992) 311.
[15] D. Calzetti, M. Giavalisco, R. Ruffini, G. Wiedenmann, Astron. Astrophys. 251 (1991) 385.
[16] B.J.T. Jones, V.J. Martinez, S.E.J. Einasto, Astrophys. J. 332 (1988) L1.
[17] H. Atmanspacher, H. Scheingraber, G. Weidenmann, Phys. Rev. A 40 (1989) 3954.

[18] P. Garrido, S. Lovejoy, D. Schertzer, Physica A 225 (1996) 294–311.
[19] V. Martinez, Vista Astron. 33 (1990) 337.
[20] F. Sylos Labini, L. Pietronero, Astrophys. J. 469 (1996) 28.
[21] F. Sylos Labini, A. Gabrielli, M. Montuori, L. Pietronero, Physica A 226 (1996) 195–242.
[22] D. Schertzer, S. Lovejoy, in: L. Pietronero (Ed.), Fractals: Physical Origin and Consequences, Plenum press, New York, 1989, p. 49.
[23] D. Lavallée, S. Lovejoy, D. Schertzer, in: D. Schertzer, S. Lovejoy (Eds.), Non-linear Variability in Geophysics: Scaling and Fractals, Kluwer, Dordrecht, 1991, pp. 99–110.
[24] M. Geller, J. Huchra, Astrophys. J. Suppl. 52 (1983) 61.
[25] J. Huchra, M. Davis, D. Latham, J. Tonry, Astrophys. J. Suppl. 52 (1983) 89.
[26] B.B. Mandelbrot, Fractals, Form, Chance and Dimension, Freeman, San Francisco, 1977.
[27] A.S. Monin, A.M. Yaglom, Statistical Fluid Mechanics, MIT Press, Cambridge, MA, 1975.
[28] P. Schecter, Astrophys. J. 203 (1976) 297.
[29] E. Hubble, Ap. J. 64 (1926) 321.
[30] P.M. Garnavitch, Astrophys. J. 493 (1997) L53.